San Luis Valley, COLORADO, UNITED STATES

HeliFALCON™ Airborne Gravity Gradiometer Survey

for
USGS

Logistics and Processing Report

Survey Flown: February, 2012

By

FUGRO AIRBORNE SURVEYS CORP
2505 Meadowvale Blvd.
Mississauga, Ontario, L5N 5S2
CANADA

Job# 11088

TABLE OF CONTENTS

1 INTRODUCTION 5
1.1 Survey Location 5
1.2 General Disclaimer 6
2 SUMMARY OF SURVEY PARAMETERS 7
2.1 Survey Area Specifications 7
2.2 Data Recording 7
2.3 Job Safety Plan, HSE Summary 8
3 FIELD OPERATIONS 9
3.1 Operations 9
3.2 Base Stations 9
3.3 Field Personnel 9
4 QUALITY CONTROL RESULTS 10
4.1 Survey acquisition issues 10
4.2 Flight Path Map 11
4.3 Turbulence 13
4.4 AGG System Noise 15
4.5 Digital Terrain Model 20
4.6 Terrain Clearance 23
5 HeliFALCON™ AIRBORNE GRAVITY GRADIENT (AGG) RESULTS 25
5.1 Processing Summary 25
5.2 HeliFALCON™ Airborne Gravity Gradiometer Data 25
5.3 Radar Altimeter Data 26
5.4 Laser Scanner Data 26
5.5 Positional Data 26
5.6 Additional Processing 26
5.7 HeliFALCON™ Airborne Gravity Gradient Data - G_{DD} & g_D 27
5.7.1 Fourier 27
5.7.2 Equivalent Source 27
5.7.3 Drape Surfaces 27
5.7.4 Fourier and Equivalent Source Maps 27
5.8 Conforming g_D to regional gravity 36
6 APPENDIX I - SURVEY EQUIPMENT 41
6.1 Survey Aircraft 41
6.2 HeliFALCON™ Airborne Gravity Gradiometer 41
6.3 Airborne Data Acquisition Systems 41
6.4 Real-Time Differential GPS 41
6.5 GPS Base Station Receiver 41
6.6 Altimeters 42
6.7 Laser Scanner 42
6.8 Data Processing Hardware and Software 42
7 APPENDIX II - SYSTEM TESTS 43
7.1 Instrumentation Lag 43
7.2 Radar Altimeter Calibration 43
7.3 HeliFALCON™ AGG Noise Measurement 43
7.4 Daily Calibrations 43
7.4.1 HeliFALCON™ AGG Calibration 43
8 APPENDIX III - HeliFALCON™ AGG DATA & PROCESSING 44
8.1 Nomenclature 44
8.2 Units 44
8.3 HeliFALCON™ Airborne Gravity Gradiometer Surveys 44
8.4 Gravity Data Processing 44

8.5 Aircraft dynamic corrections 45
8.6 Self gradient Corrections 45
8.7 Laser Scanner Processing 45
8.8 Terrain Corrections 45
8.9 Tie-line Levelling 46
8.10 Transformation into G_{DD} & g_D 46
8.11 Noise & Signal 46
8.12 Risk Criteria in Interpretation 47
8.13 References 47
9 APPENDIX IV - FINAL PRODUCTS 49

FIGURES

Figure 1: San Luis Valley, CO, United States – *Survey Area Location* 5
Figure 2: Block 1 – *Flight Path map* 11
Figure 3: Block 2 – *Flight Path map* 12
Figure 4: Block 1 – *Turbulence (milli g where g = 9.80665 m/sec/sec)* 13
Figure 5: Block 2 – *Turbulence (milli g where g = 9.80665 m/sec/sec)* 14
Figure 6: Block 1 – *System Noise NE (*E*)* 16
Figure 7: Block 2 – *System Noise NE (*E*)* 17
Figure 8: Block 1 – *System Noise UV (*E*)* 18
Figure 9: Block 2 – *System Noise UV (*E*)* 19
Figure 10: Block 1 – *Final Digital Terrain Model (metres, referenced to the EGM96 geoid)* 21
Figure 11: Block 2 – *Final Digital Terrain Model (metres, referenced to the EGM96 geoid)* 22
Figure 12: Block 1 – *Terrain Clearance from laser scanner data (metres above ground surface)* 23
Figure 13: Block 2 – *Terrain Clearance from laser scanner data (metres above ground surface)* 24
Figure 14: *FALCON™ AGG Data Processing* 25
Figure 15: Block 1 – *Vertical Gravity Gradient (G_{DD}) from Fourier processing (E).* 28
Figure 16: Block 2 – *Vertical Gravity Gradient (G_{DD}) from Fourier processing (E).* 29
Figure 17: Block 1 – *Vertical Gravity Gradient (G_{DD}) from equivalent source processing (E).* 30
Figure 18: Block 2 – *Vertical Gravity Gradient (G_{DD}) from equivalent source processing (E).* 31
Figure 19: Block 1 – *Vertical Gravity (g_D) from Fourier processing (mGal)* 32
Figure 20: Block 2– *Vertical Gravity (g_D) from Fourier processing (mGal)* 33
Figure 21: Block 1 – *Vertical Gravity (g_D) from equivalent source processing (mGal)* 34
Figure 22: Block 2 – *Vertical Gravity (g_D) from equivalent source processing (mGal)* 35
Figure 23: Block 1 – *Vertical Gravity (g_D) from Fourier processing conformed to regional gravity data (mGal)* 37
Figure 24: Block 2 – *Vertical Gravity (g_D) from Fourier processing conformed to regional gravity data (mGal)* 38
Figure 25: Block 1 – *Vertical Gravity (g_D) from equivalent source processing conformed to regional gravity data (mGal).* 39
Figure 26: Block 2 – *Vertical Gravity (g_D) from equivalent source processing conformed to regional gravity data (mGal).* 40

TABLES

Table 1: Block 1 – *Survey Boundary Coordinates* 7
Table 2: Block 2 – *Survey Boundary Coordinates* 7
Table 3: Final HeliFALCON™ AGG Digital Data – *Geosoft Database Format* 52
Table 4: Final AGG Grids – *Geosoft GRD Format* 53

1 INTRODUCTION

Fugro Airborne Surveys conducted a high-sensitivity HeliFALCON™ Airborne Gravity Gradiometer (AGG) survey over the Block 1 (main area) and Block 2 (smaller area) survey areas under contract with United States Geological Survey.

1.1 Survey Location

The Block 1 and Block 2 survey areas are centred on longitude 105° 33´ W , latitude 37º 45' N (see the location map in *Figure 1*).

The production flights took place during February 2012 with the first production flight taking place on February 10th and the final flight taking place on February 20th. To complete the survey area coverage a total of 14 production flights were flown, for a combined total of 1975 line kilometres of data acquired.

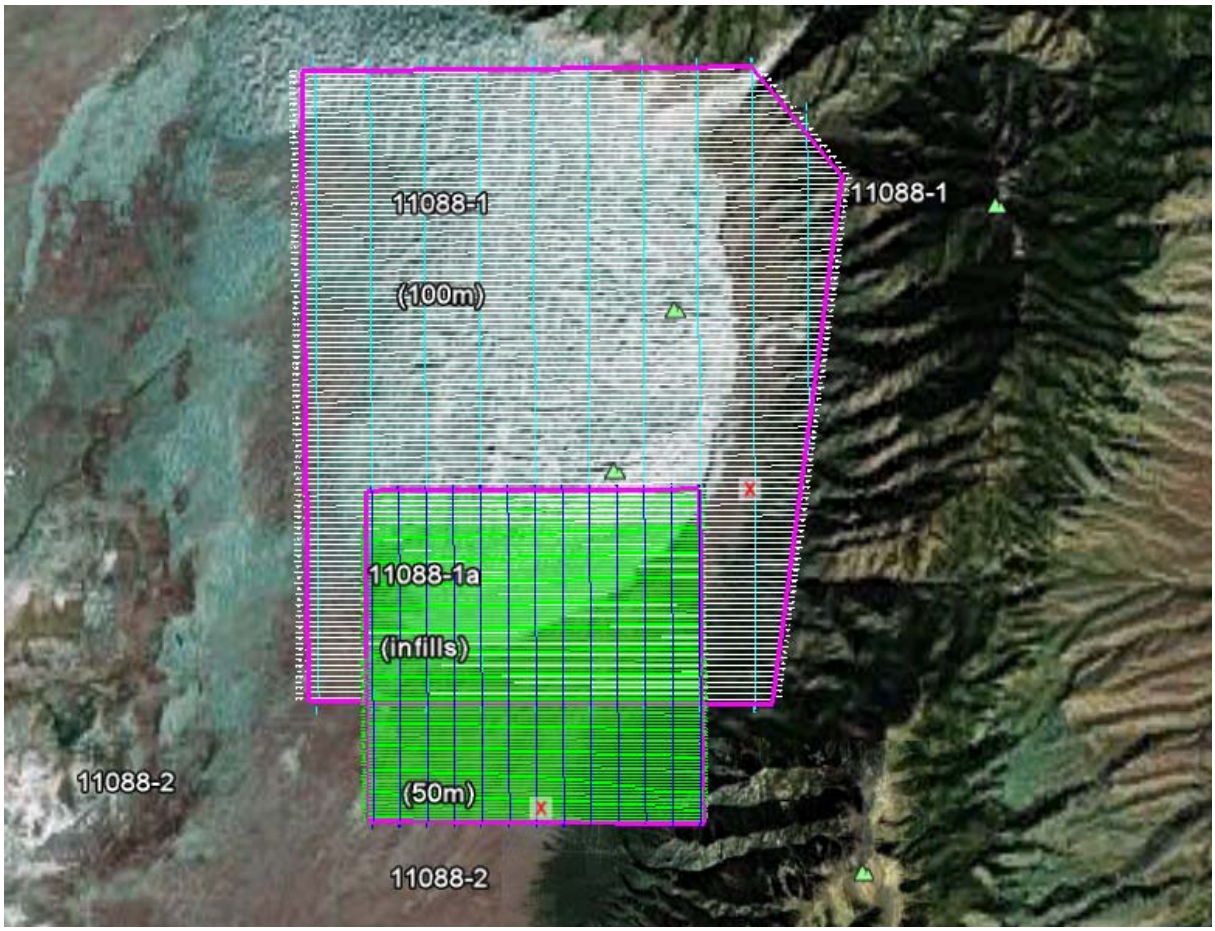

Figure 1: San Luis Valley, CO, United States – *Survey Area Location*

1.2 General Disclaimer

It is Fugro Airborne Survey's understanding that the data and report provided to the client is to be used for the purpose agreed between the parties. That purpose was a significant factor in determining the scope and level of the Services being offered to the Client. Should the purpose for which the data and report is used change, the data and report may no longer be valid or appropriate and any further use of, or reliance upon, the data and report in those circumstances by the Client without Fugro Airborne Survey's review and advice shall be at the Client's own or sole risk.

The Services were performed by Fugro Airborne Survey exclusively for the purposes of the Client. Should the data and report be made available in whole or part to any third party, and such party relies thereon, that party does so wholly at its own and sole risk and Fugro Airborne Survey disclaims any liability to such party.

Where the Services have involved Fugro Airborne Survey's use of any information provided by the Client or third parties, upon which Fugro Airborne Survey was reasonably entitled to rely, then the Services are limited by the accuracy of such information. Fugro Airborne Survey is not liable for any inaccuracies (including any incompleteness) in the said information, save as otherwise provided in the terms of the contract between the Client and Fugro Airborne Survey.

2 SUMMARY OF SURVEY PARAMETERS

2.1 Survey Area Specifications

Block 1 (Main Area)

Total Kilometres (km)	1162.4
Minimum Drape Height (m)	80
Clearance Method	Contour
Traverse Line Direction (deg.)	E-W (90°-270°)
Traverse Line Spacing (m)	100
Tie Line Direction (deg.)	N-S (0°-180°)
Tie Line Spacing (m)	1000

Block 2 (Smaller Area)

Total Kilometres (km)	812.2
Minimum Drape Height (m)	40
Clearance Method	Contour
Traverse Line Direction (deg.)	E-W (90°-270°)
Traverse Line Spacing (m)	50
Tie Line Direction (deg.)	N-S (0°-180°)
Tie Line Spacing (m)	500

The survey blocks are defined by the coordinates in *Table 1* and *Table 2*, in UTM Zone 13N projection, referenced to the WGS84 datum

Corner Number	Easting	Northing
1	447331	4185374
2	455583	4185357
3	457205	4183383
4	455875	4173835
5	447392	4173855

Table 1: Block 1 – *Survey Boundary Coordinates*

Corner Number	Easting	Northing
1	448491	4177704
2	454594	4177707
3	454622	4171677
4	448495	4171674
5	448491	4177704

Table 2: Block 2 – *Survey Boundary Coordinates*

2.2 Data Recording

The following parameters were recorded during the course of the survey:

- **HeliFALCON™ AGG data:** recorded at different intervals.
- **Terrain clearance:** provided by the radar altimeter at intervals of 0.1 s.
- **Airborne GPS positional data** (latitude, longitude, height, time and raw range from each satellite being tracked): recorded at intervals of 1 s.
- **Time markers:** in digital data.

- **Ground based GPS positional data** (latitude, longitude, height, time and raw range from each satellite being tracked): recorded at intervals of 1 s.
- **Aircraft distance to ground:** measured by two laser scanners, scanning at 20 times per second (when in range of the instrument and in the absence of thick vegetation).

2.3 Project Safety Plan, HSE Summary

A Project Safety Plan was prepared and implemented in accordance with the Fugro Airborne Surveys Occupational Safety and Health Management System.

3 FIELD OPERATIONS

3.1 Operations

The survey was based out of Alamosa, Colorado, USA. The survey aircraft was operated from **KALS** San Luis Valley Regional Airport/Bergman Field, Alamosa, Colorado, USA using aircraft fuel available on site. A temporary office was set up in Alamosa, CO where all survey operations were run and the post-flight data verification was performed.

3.2 Base Stations

A dual frequency GPS base station was set up close to the blocks (less then 35 km) in order to correct the raw GPS data collected in the aircraft. A secondary GPS base station was available and set up at the Airport, but was not required.

GPS Base Stations

Block 1 and Block 2

Valid for Flight FLT002

Date:	February 08 to February 20, 2012
Location:	San Luis Valley Airport, CO, US
Latitude:	37 26 29.3928N
Longitude:	105 52 03.7249W
Height:	2282.288 m ellipsoidal

Valid for Flights FLT003 to FLT015

Date:	February 10 to February 20, 2012
Location:	Great Sands Dune Oasis Park, CO, US
Latitude:	37 43 32.0996 N
Longitude:	105 31 09.5640W
Height:	2463.213 m ellipsoidal

3.3 Field Personnel

The following technical personnel participated in field operations:

Crew Leader/Processor:	Mihai Szentesy and Michael Wu
Pilots:	Daniel Ragan
Technicians:	Burke Schieman, Ji Yun Baik and Logan Streun
Project Manager:	Lesley Minty
Final QC and Processing:	Peter Chambers

4 QUALITY CONTROL RESULTS

4.1 Survey acquisition issues

During the course of the survey there were no data quality issues with:

AGG instrumentation
GPS base stations
Data acquisition systems
Radar altimeter
Laser scanner

4.2 Flight Path Map

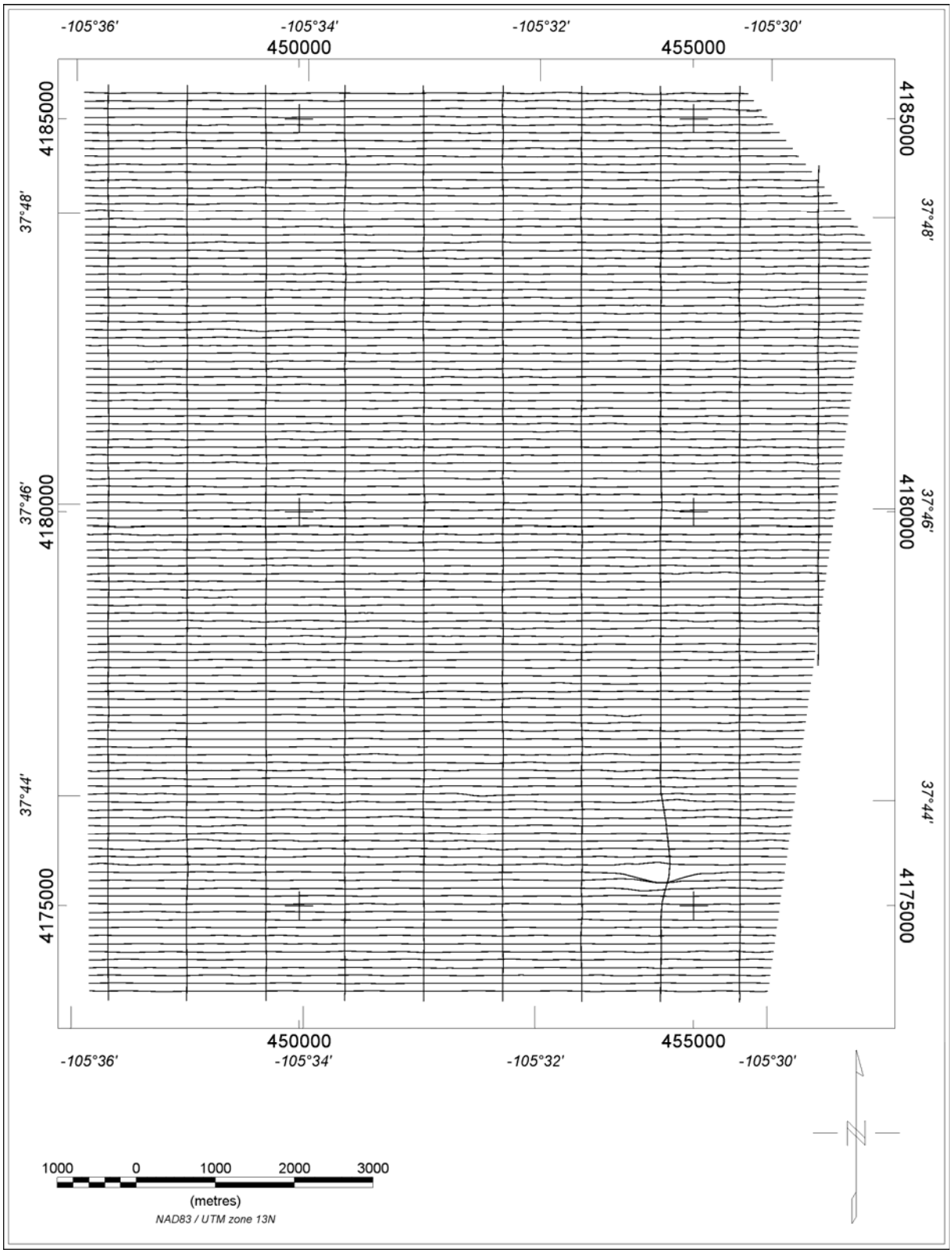

Figure 2: Block 1 – *Flight Path map*

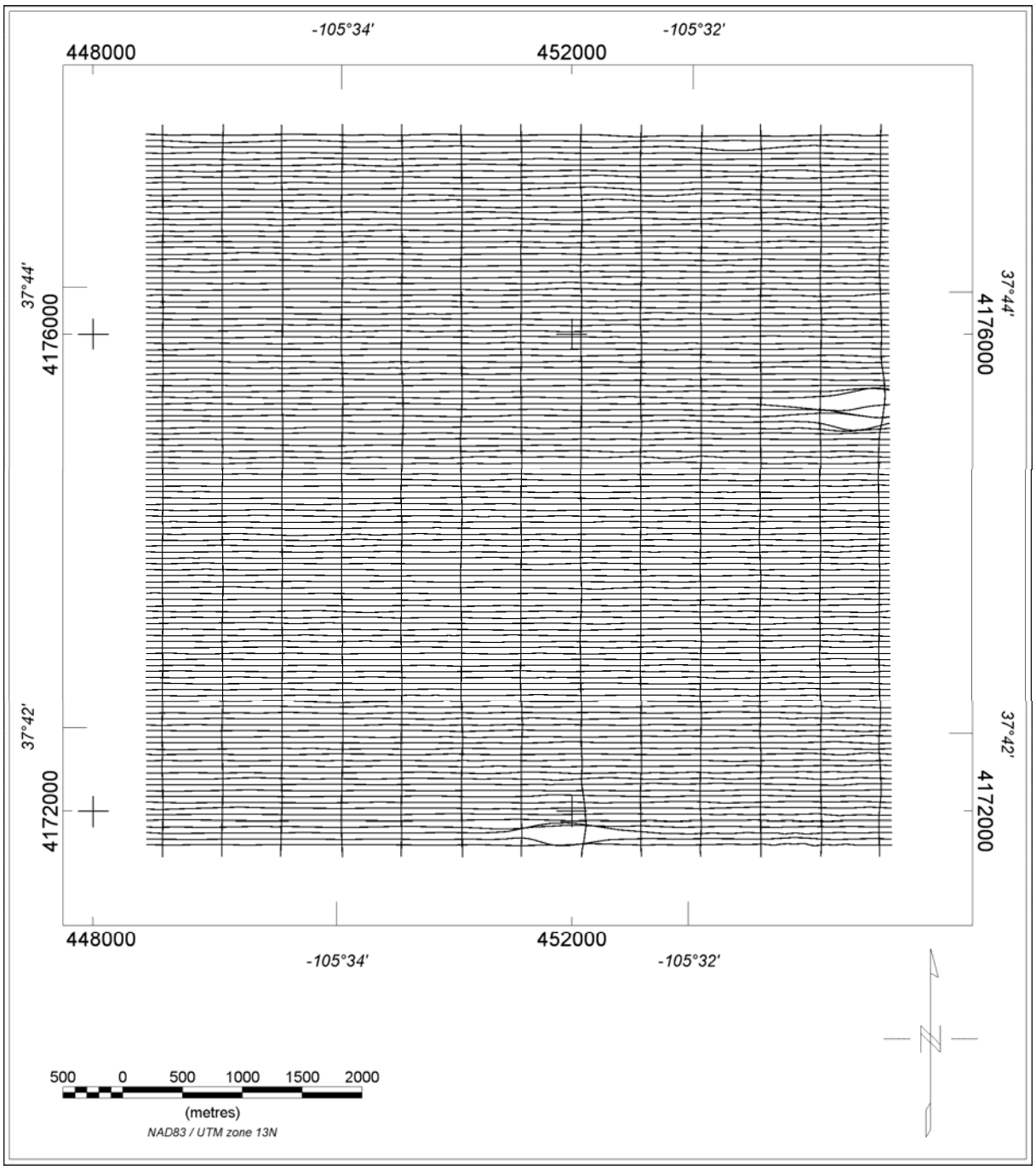

Figure 3: Block 2 – *Flight Path map*

4.3 Turbulence

The mean turbulence recorded across the survey areas was 25.0 milli g (where g = 9.80665 m/sec/sec) in Block 1 and 26.4 in Block 2. Turbulence was generally low throughout most of the job and the most variation occurred with the changes in daily weather conditions. The turbulence pattern across the survey areas is shown in *Figure 4* and *Figure 5*.

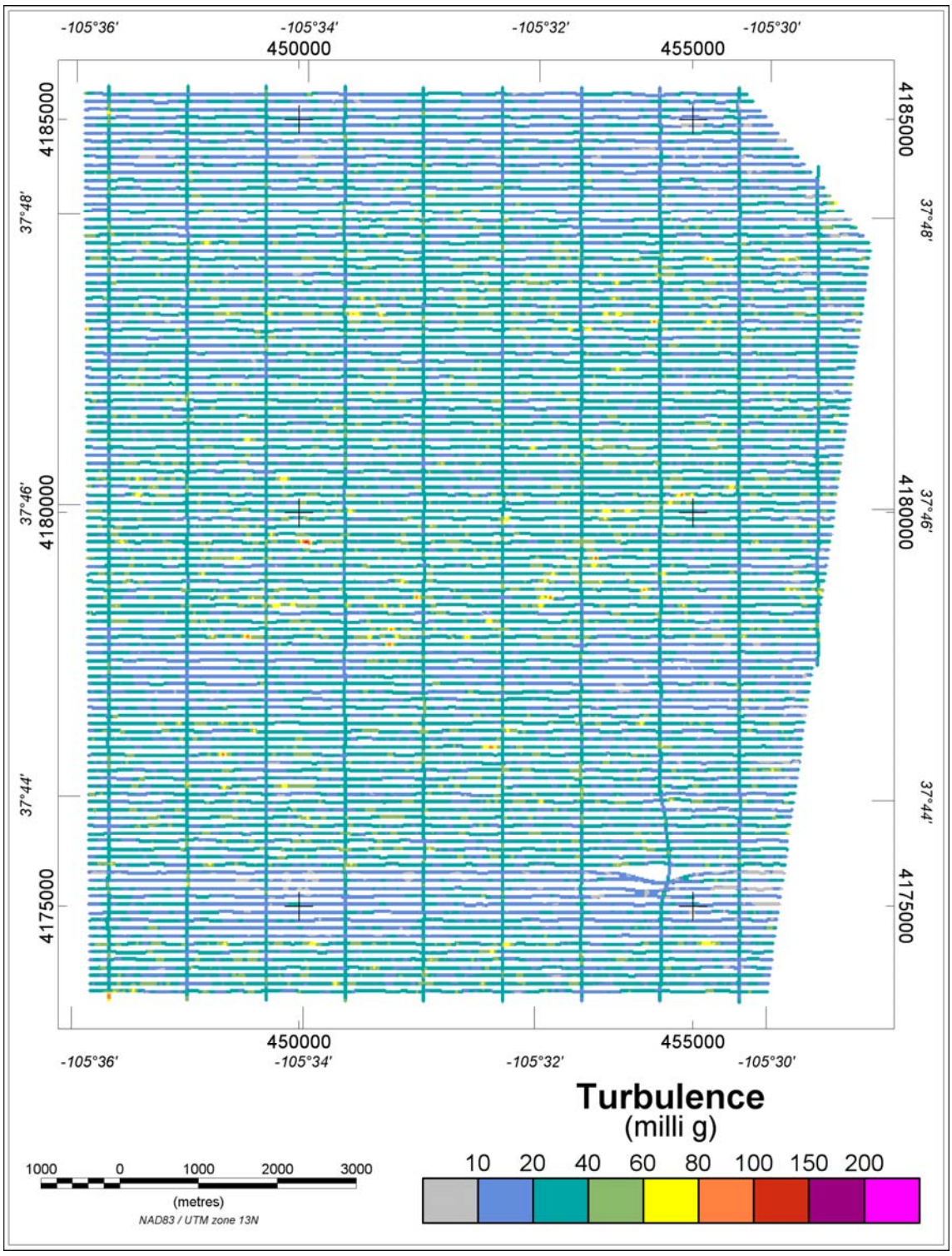

Figure 4: Block 1 – *Turbulence (milli g where g = 9.80665 m/sec/sec)*

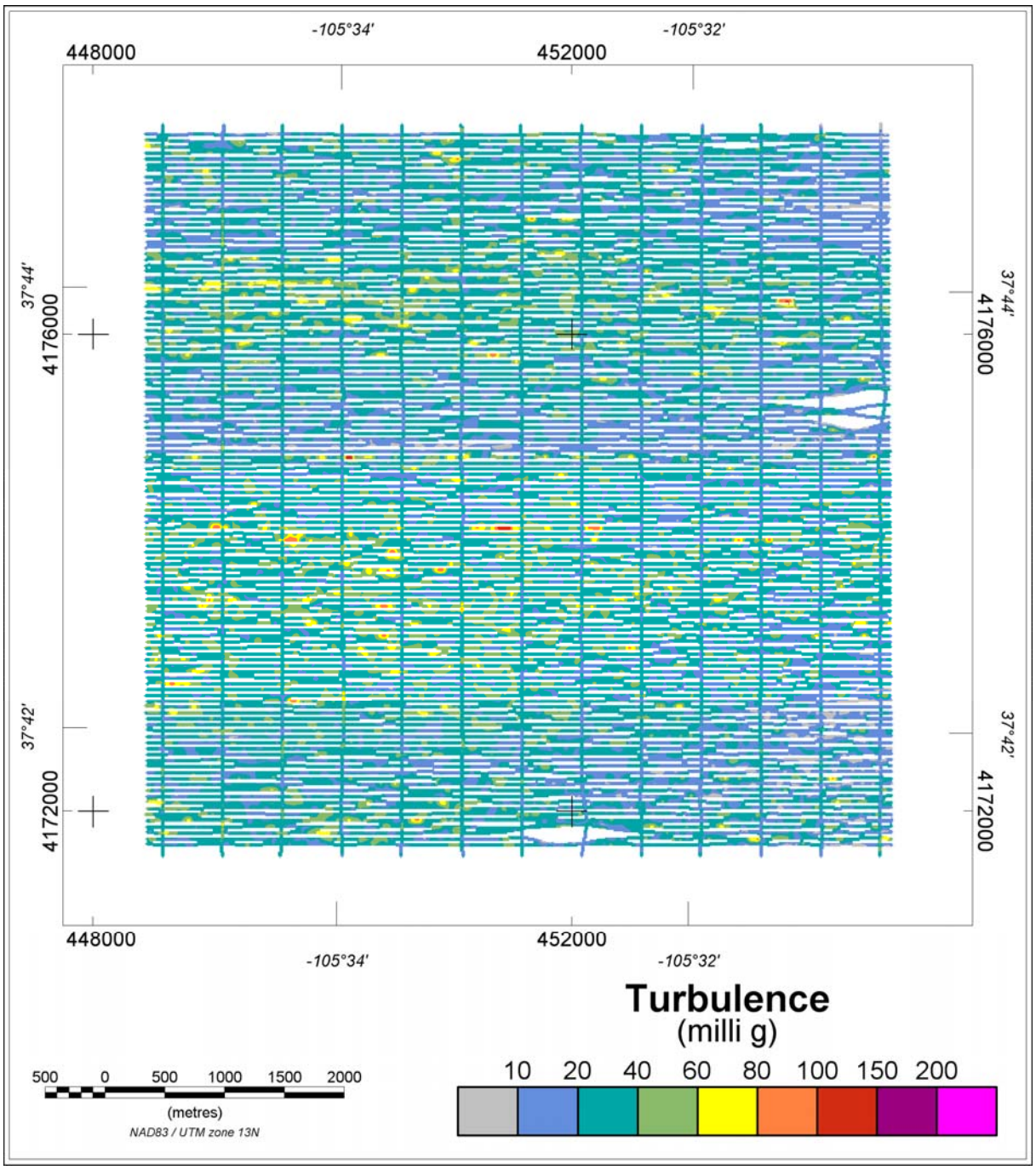

Figure 5: Block 2 – *Turbulence (milli g where g = 9.80665 m/sec/sec)*

4.4 AGG System Noise

The system noise is defined to be the standard deviation of half the difference between the A & B complements, for each of the NE and UV curvature components. The results for this survey were very good with values of 2.78 E and 2.89 E for NE and UV respectively for Block 1 and values of 2.88 E and 3.04 E for NE and UV respectively for Block 2.

Figure 6, *Figure 7*, *Figure 8* and *Figure 9* provide a representation of the variation in this standard deviation for each component. This is achieved by gridding a rolling measurement of standard deviation along each line using a window length of 100 data points.

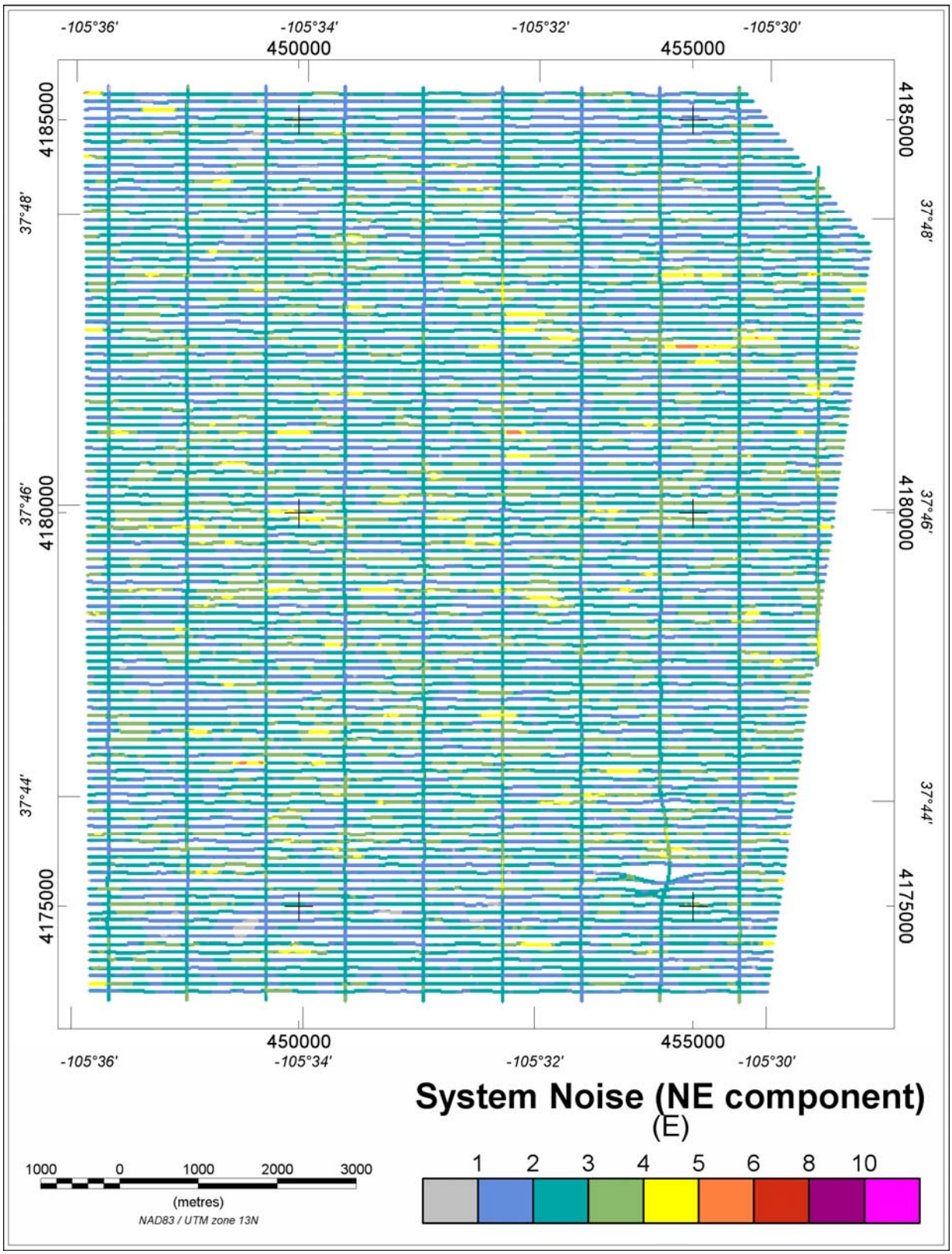

Figure 6: Block 1 – *System Noise NE (*E*)*

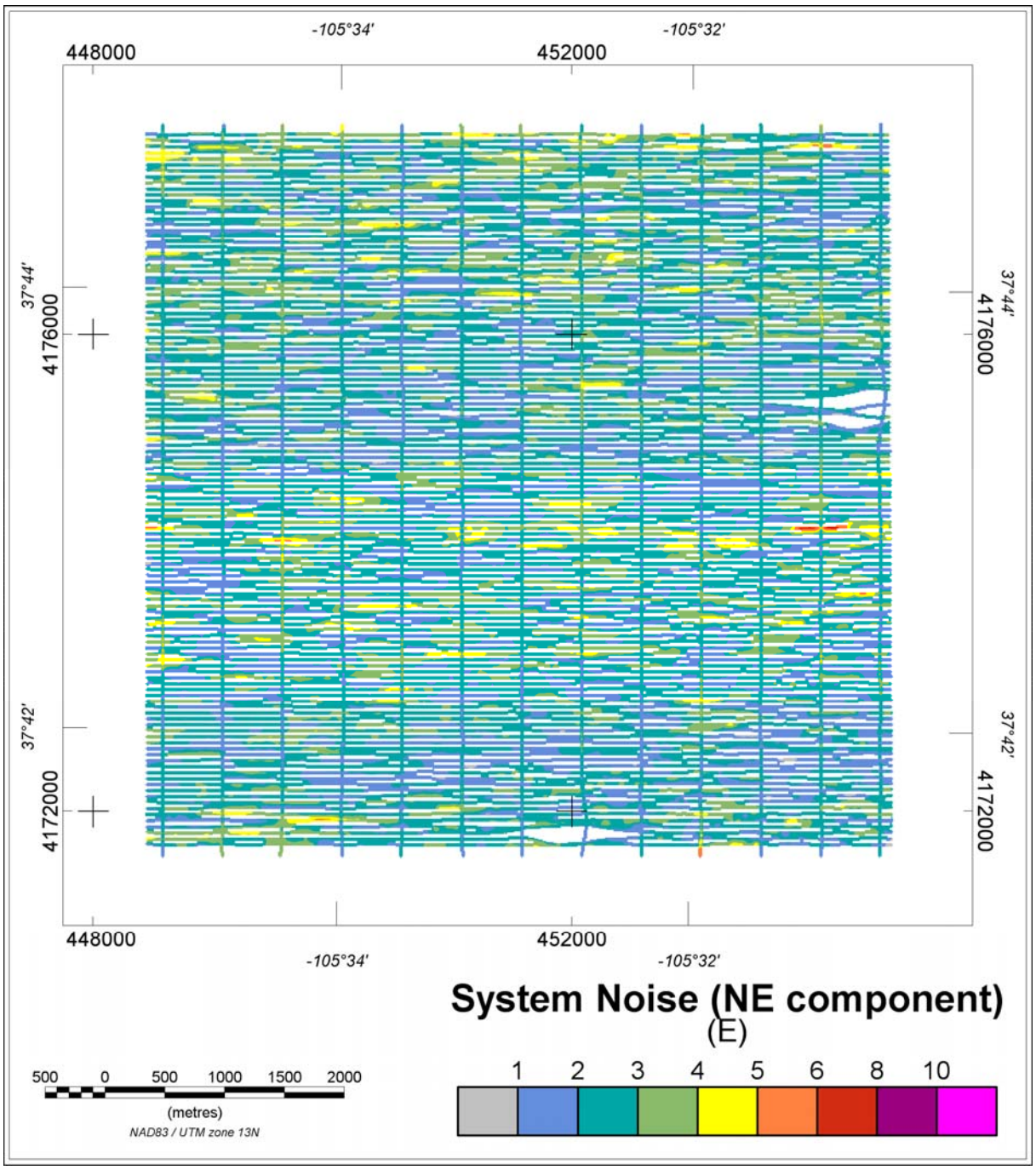

Figure 7: Block 2 – *System Noise NE (*E*)*

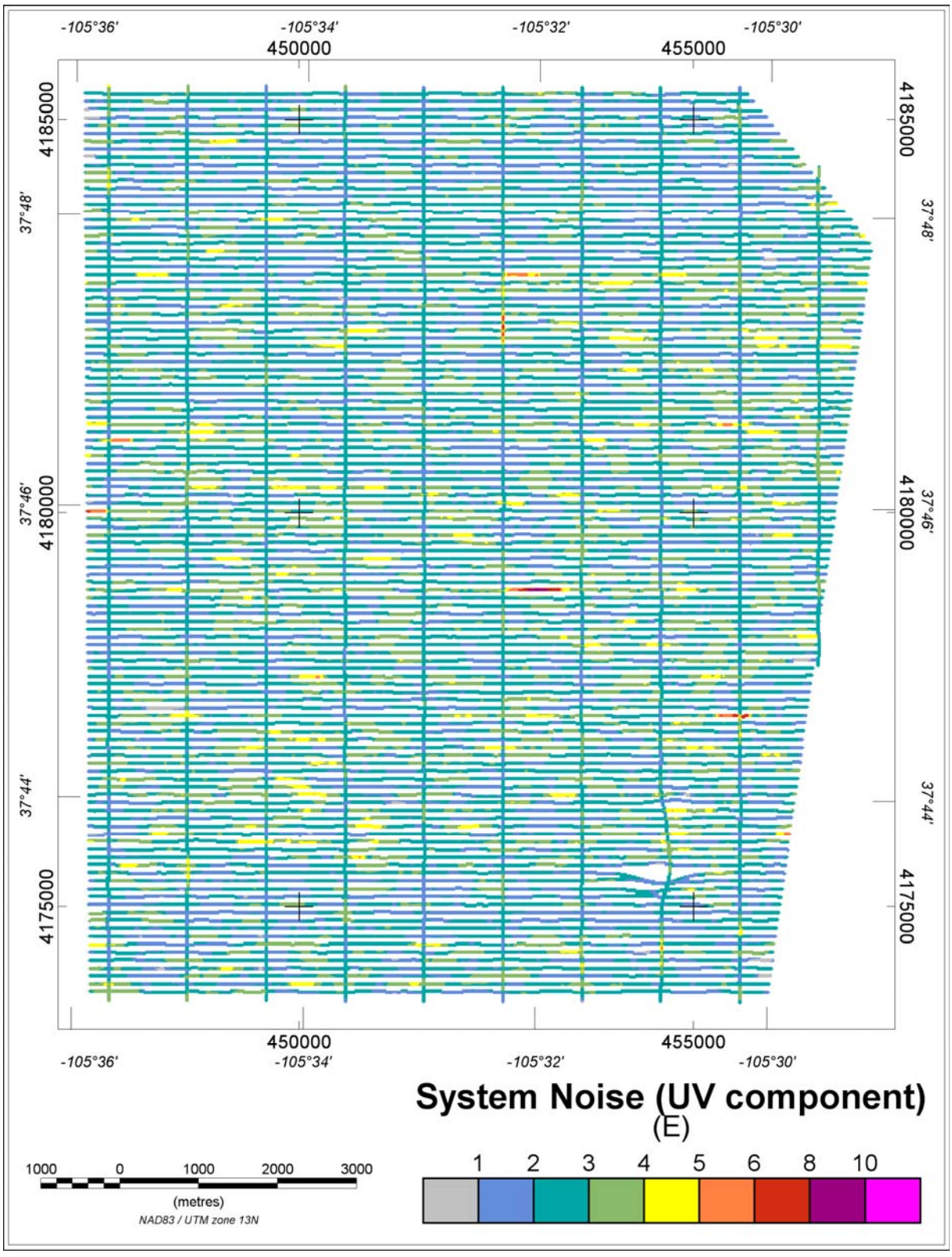

Figure 8: Block 1 – *System Noise UV (*E*)*

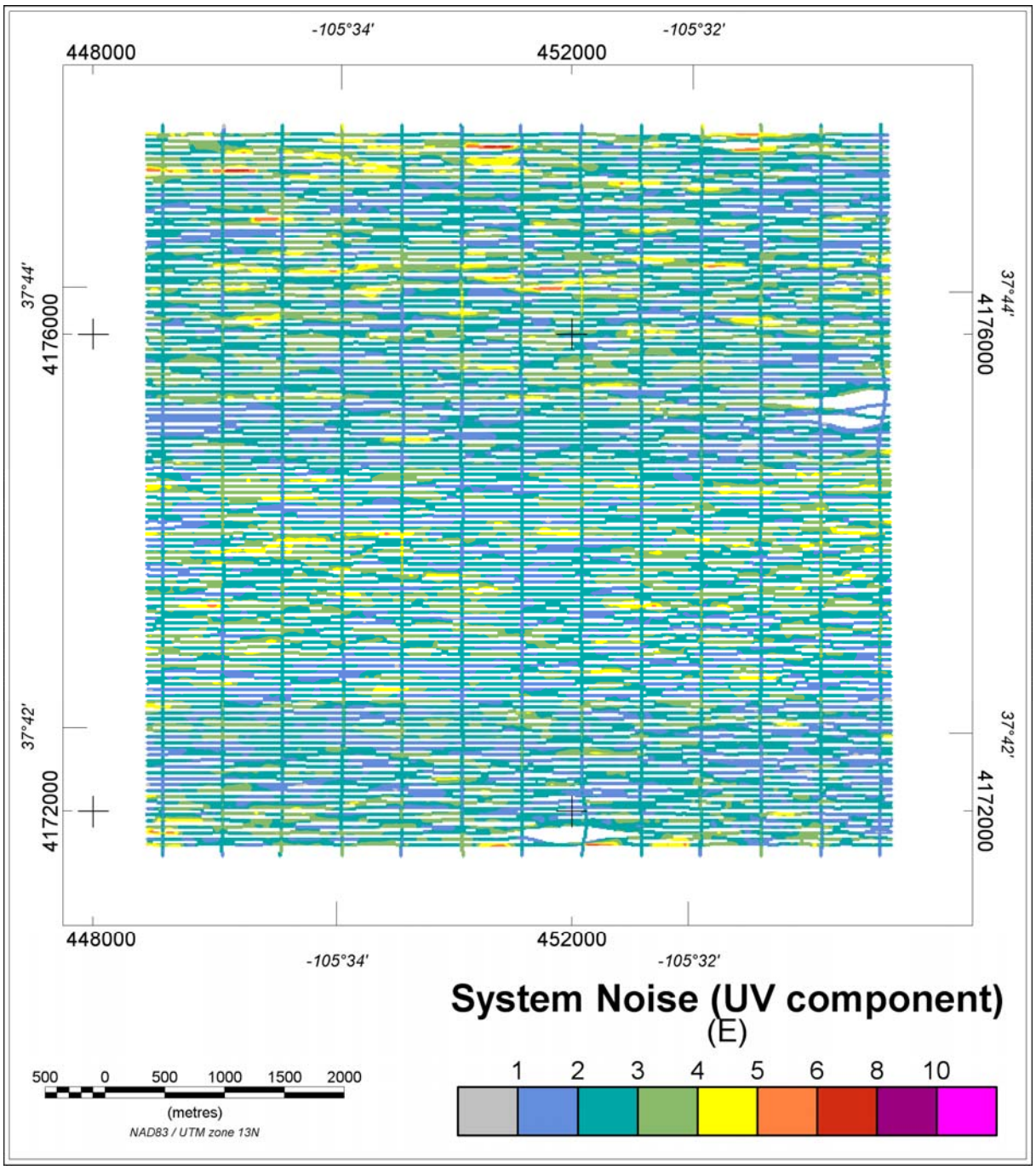

Figure 9: Block 2 – *System Noise UV (*E*)*

4.5 Digital Terrain Model

Laser scanner range data were combined with GPS position and height data (adjusted from height above the WGS84 ellipsoid to height above the geoid by applying the Earth Gravitational Model 1996 (EGM96)). The outputs of this process are two “swaths” of terrain elevations extending either side of the aircraft flight path. Width and sample density of this swath varies with aircraft height. Typical values are 100 to 150 metres and 5 to 10 metres respectively.

Because terrain correction of AGG data requires knowledge of the terrain at distances up to at least 10 km from the data location, laser scanner data collected only along the survey line path must be supplemented by data from another source. For this purpose, Shuttle Radar Topography Mission (SRTM) v2 (high resolution, one arc second) data were used.

Laser scanner data quality was very good with scan density generally above 90%. Laser scanner data were gridded at 10 m with a 1 cell maximum extension beyond data limits. The gaps were then filled using a Fourier domain data wrapping approach. To supplement the laser data, the SRTM data were excised to an area 15 km beyond the survey area. The excised data were filled using the same Fourier domain wrapping method, then adjusted to the level of the laser scanner data prior to merging.

Figure 10 and *Figure 11* show the final Digital Terrain Model for each area resulting from the laser scanner and SRTM data processing.

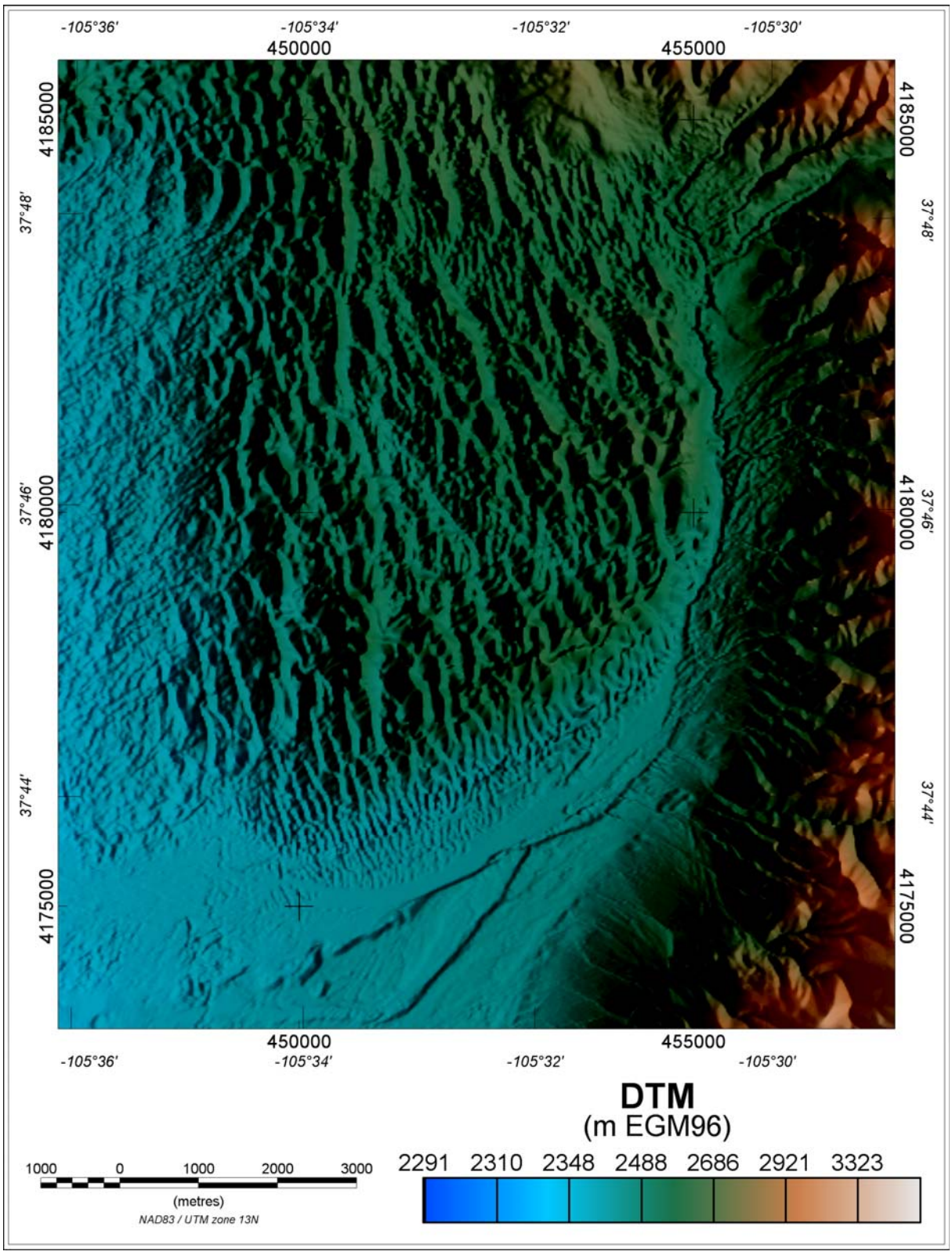

Figure 10: Block 1 – *Final Digital Terrain Model (metres, referenced to the EGM96 geoid)*

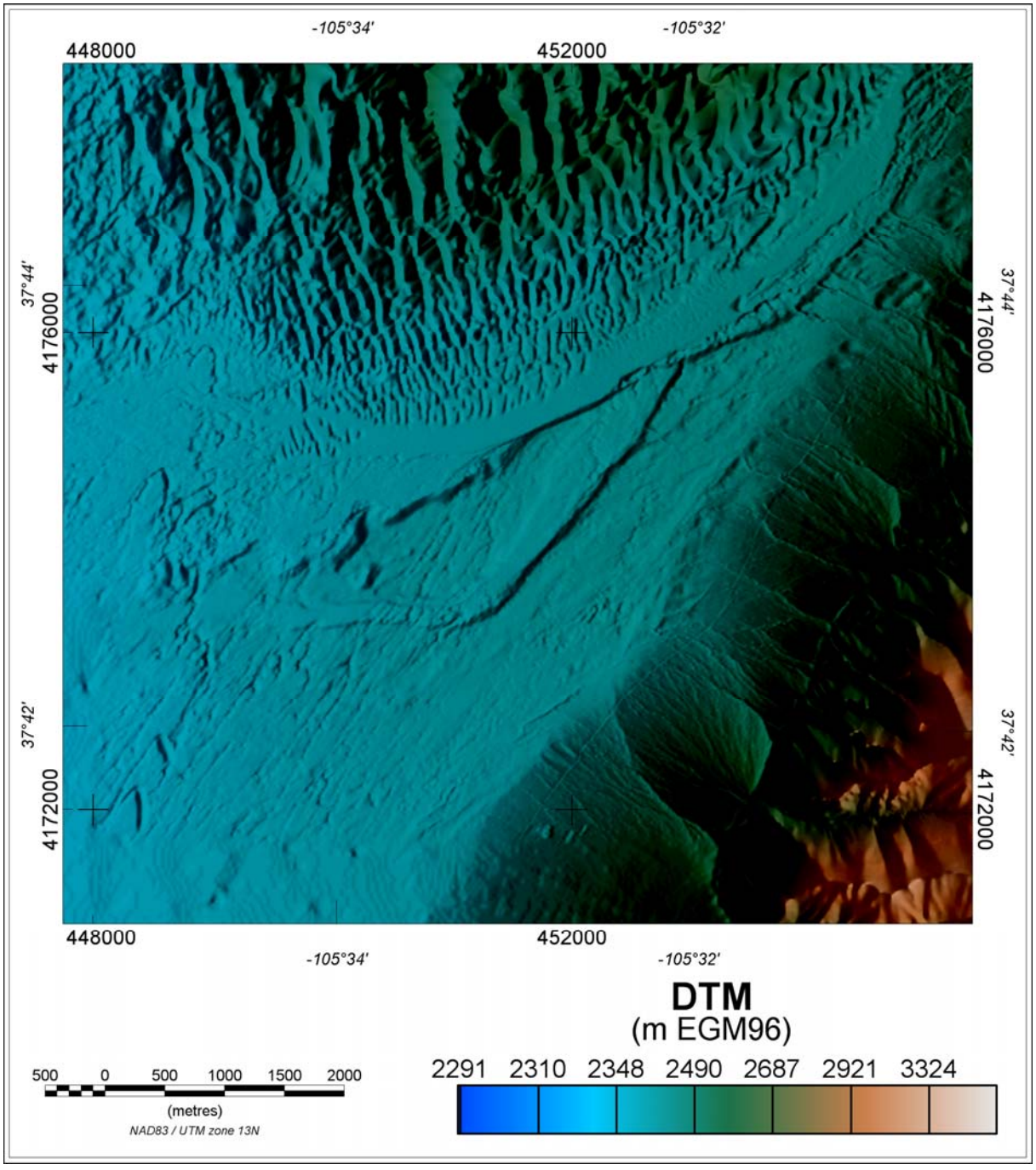

Figure 11: Block 2 – *Final Digital Terrain Model (metres, referenced to the EGM96 geoid)*

4.6 Terrain Clearance

Terrain clearance for Block 1 averaged just above the nominal clearance of 80 m having a mean value of 81 m and averaged 46 m for Block 2, a little above the nominal clearance of 40 m across the survey area. The terrain clearances, as derived from laser scanner data and GPS altitude, are shown in *Figure 12* and *Figure 13*.

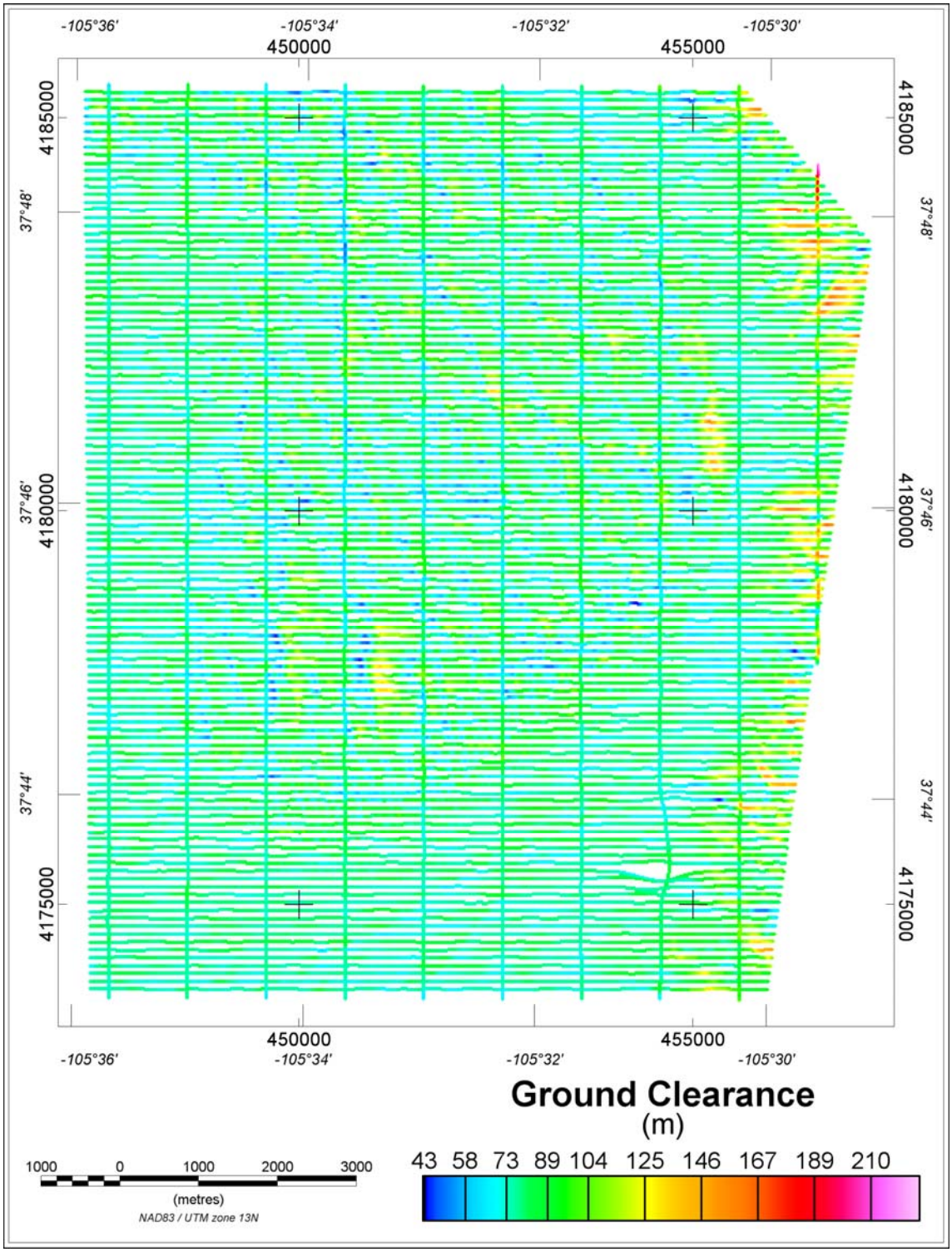

Figure 12: Block 1 – *Terrain Clearance from laser scanner data (metres above ground surface)*

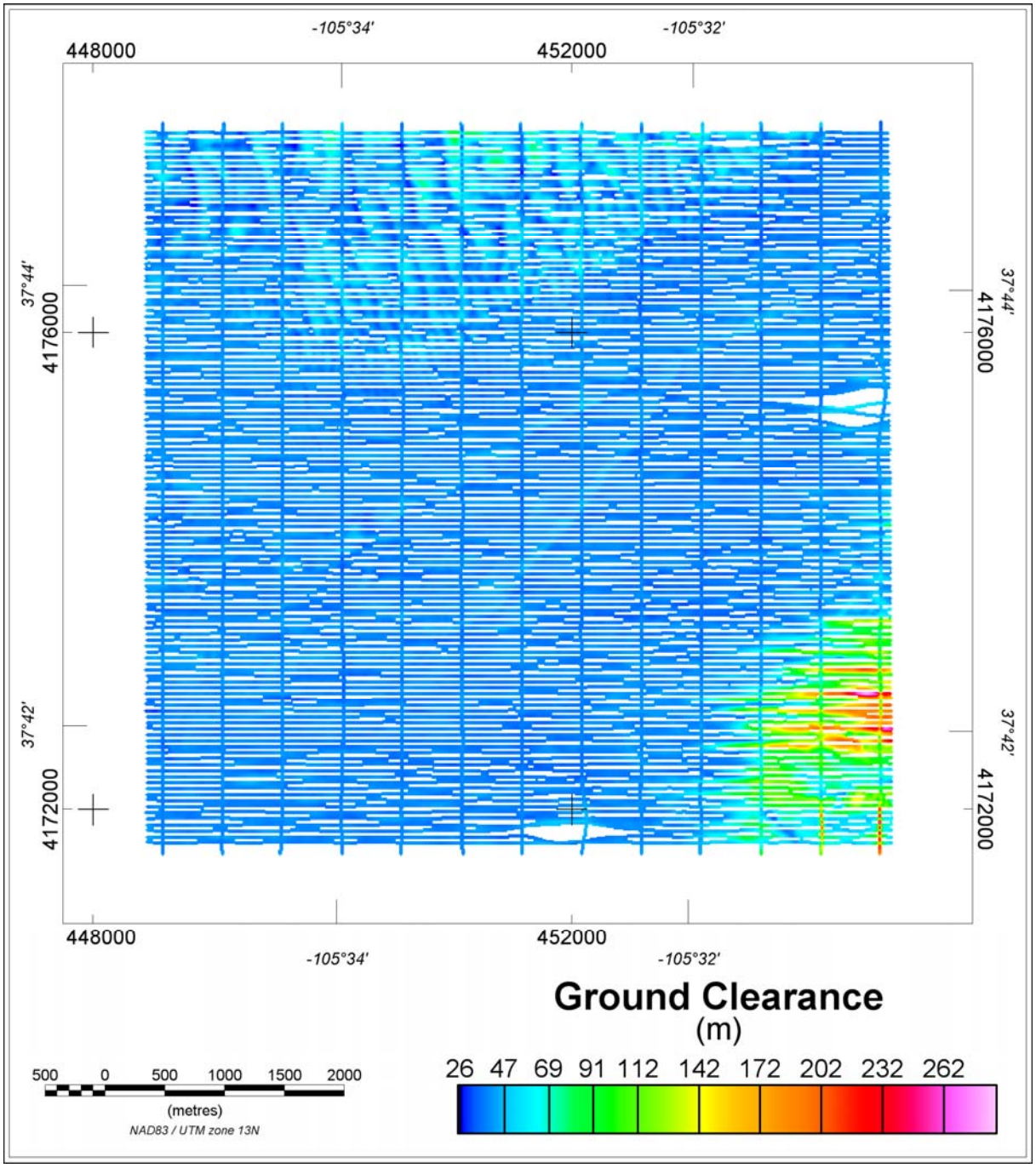

Figure 13: Block 2 – *Terrain Clearance from laser scanner data (metres above ground surface)*

5 HeliFALCON™ AIRBORNE GRAVITY GRADIENT (AGG) RESULTS

5.1 Processing Summary

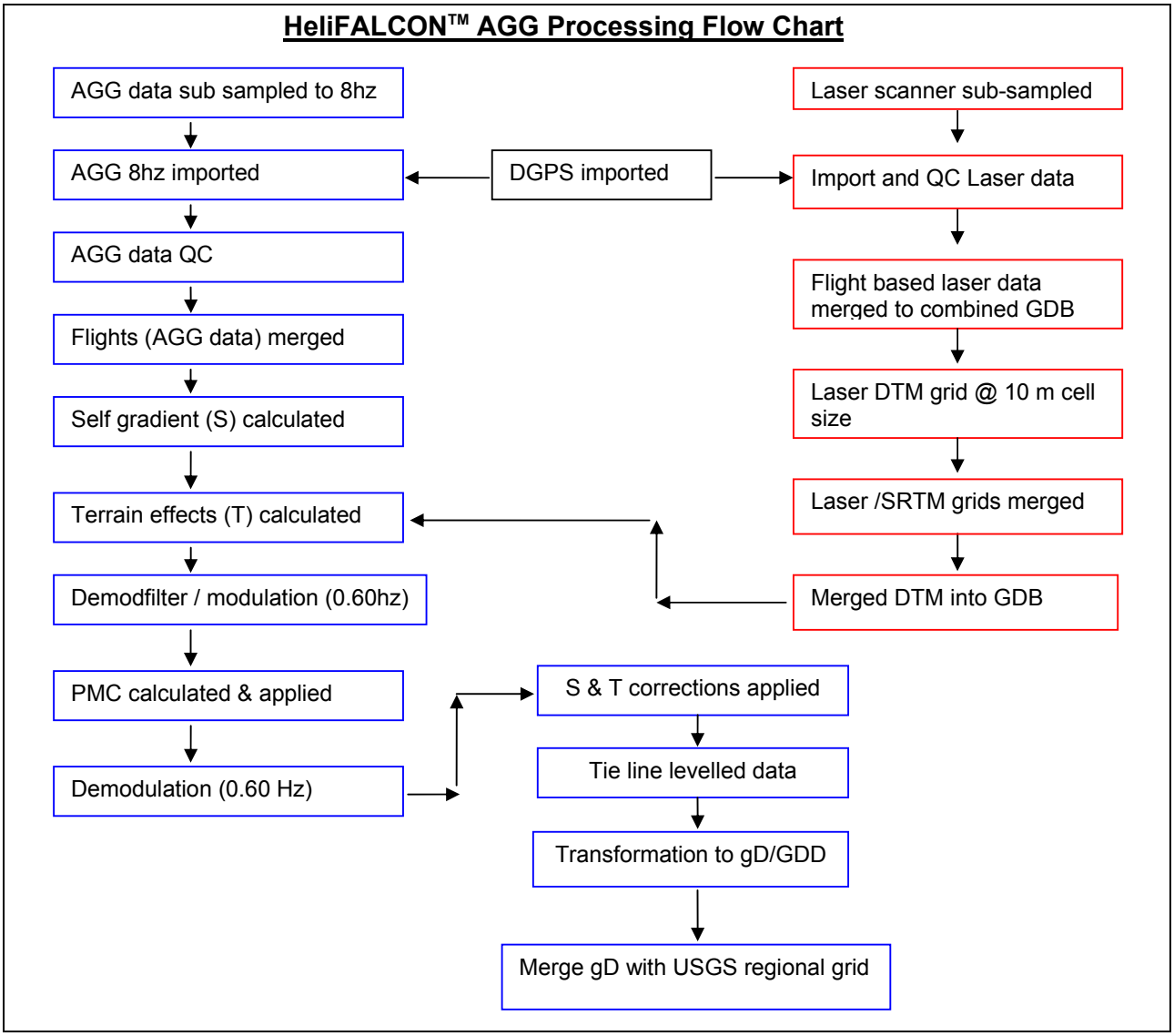

Figure 14: ***FALCON™*** *AGG Data Processing*

5.2 HeliFALCON™ Airborne Gravity Gradiometer Data

Figure 14 summarises the steps involved in processing the AGG data obtained from the survey.

The **HeliFALCON™** Airborne Gravity Gradiometer data were digitally recorded by the ADAS on removable hard drives. The raw data were then copied on to the field processing laptop, backed up twice onto DVD+R media and shipped to Fugro Perth using a secure courier service.

Preliminary processing and QC of the **HeliFALCON™** AGG data were completed on-site using Fugro's DiAGG software.

Further QC and Final **HeliFALCON™** AGG data processing were performed by the office based data processor.

5.3 Radar Altimeter Data

The terrain clearance measured by the radar altimeter in metres was recorded at 10 Hz. The data were plotted and inspected for quality.

5.4 Laser Scanner Data

The terrain clearance measured by the laser scanner in metres was recorded at 20 scans/sec with 276 data points per scan, and was then sub-sampled using a window width of 0.25 sec. The sub-sampled laser scanner data were edited to remove spikes prior to gridding.

5.5 Positional Data

A number of programs were executed for the compilation of navigation data in order to reformat and recalculate positions in differential mode. Waypoint's GrafNav GPS processing software was used to calculate DGPS positions from raw range data obtained from the moving (airborne) and stationary (ground) receivers.

The GPS ground station position was determined by logging GPS data continuously for 24 hours prior to survey flights commencing. The GPS data were processed and quality controlled completely in the field.

Positional data (longitude, latitude, Z) were output in the WGS84 datum. The longitude and latitude data were then projected into UTM Zone 13N coordinates.

Parameters for the WGS84 datum are:

Ellipsoid:	WGS84
Semi-major axis:	6378137.0 m
1/flattening:	298.257

All processing was performed using WGS84/UTM Zone 13N coordinates. Final line data and final grid data were supplied in NAD83/UTM Zone 13N co-ordinates.

5.6 Additional Processing

For the terrain correction, densities of 2.00 and 2.67 g/cm^3 , as requested by the USGS, were selected as approximating most closely the different regions of density of the terrain in the survey areas. As standard a density of 0 g/cm^3 (meaning no terrain correction) was also used and these data are also included. The data were tie line and micro-levelled.

5.7 HeliFALCON™ Airborne Gravity Gradient Data - G_{DD} & g_D

The transformation into G_{DD} and g_D was accomplished using two methods: Fourier domain transformation and the Method of Equivalent Sources

5.7.1 Fourier

To produce the g_D and G_{DD} grids using the standard Fourier method, the technique includes continuation to a smoothed drape surface. The drape surface is made from the altitude of the aircraft above sea level. A 2D low pass filter to improve the signal to noise ratio by removing processing artefacts and other information which is known to be beyond the sampling resolution is also applied to the Fourier data, usually with a wavelength between 1 and 2 line spacings.

For these survey blocks, the maximum amount of downward continuation is quite large compared to the line spacing (of the order of 600 m) and so the downward continuation is quite unstable. To get the downward continuation to work for block 1, a 2D cut-off wavelength of 300 m was used. For block 2 the downward continuation was too unstable to work at all so there are no grids continued to the smoothed drape surface for block 2.

For blocks 1 and 2, grids were produced without any continuation being applied. The drape surface is just the ALTITUDE surface (flying height above sea level). In the database the unsmoothed drape surface (DRAPESURFACE_FOURIER_UNSMOOTHED) is just a copy of the ALTITUDE channel. For these grids, a cut-off wavelength of 100 m for Block 1 and 50 m for Block 2 was used in the low-pass filter.

5.7.2 Equivalent Source

The equivalent source transformation utilises a smooth model inversion to calculate the density of a surface of sources followed by a forward calculation to produce g_D and G_{DD}. It was possible to match the mid to long wavelength characteristics of the Fourier results by placing the sources at a depth of 100 metres for Block 1 and 50 metres for Block 2.

5.7.3 Drape Surfaces

The drape surface information for the Fourier methods has been discussed in section 5.7.1.

The equivalent source transformation also uses a smoothed surface onto which the output data are projected. This surface is also the smoother equivalent of the actual flying surface and has been included as a database channel and as a grid.

5.7.4 Fourier and Equivalent Source Maps

The Fourier and equivalent source (density 2 g/cm^3) G_{DD} maps are shown in *Figure 15*, *Figure 16*, *Figure 17* and *Figure 18*. The Fourier maps use the grids with no continuation applied.

Two versions of vertical gravity (g_D) are presented: Fourier, derived by integrating G_{DD}; and equivalent source, derived directly from the modelled sources. The (density 2 g/cm^3) Fourier results are presented in *Figure 19* and *Figure 20* and the (density 2 g/cm^3) equivalent source results are presented in *Figure 21* and *Figure 22*. The Fourier maps use the grids with no continuation applied.

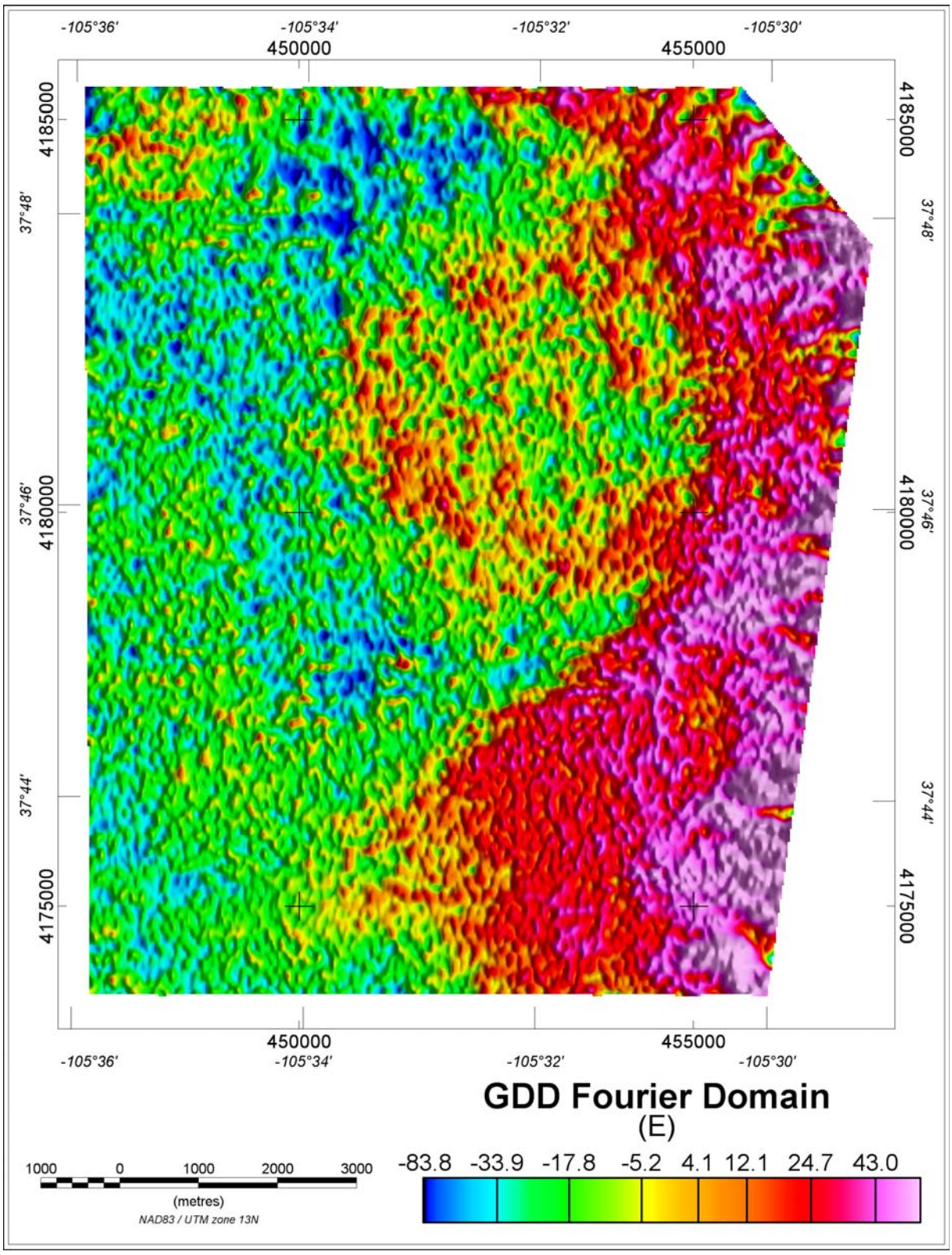

Figure 15: Block 1 – *Vertical Gravity Gradient (G_{DD}) from Fourier processing (E).*

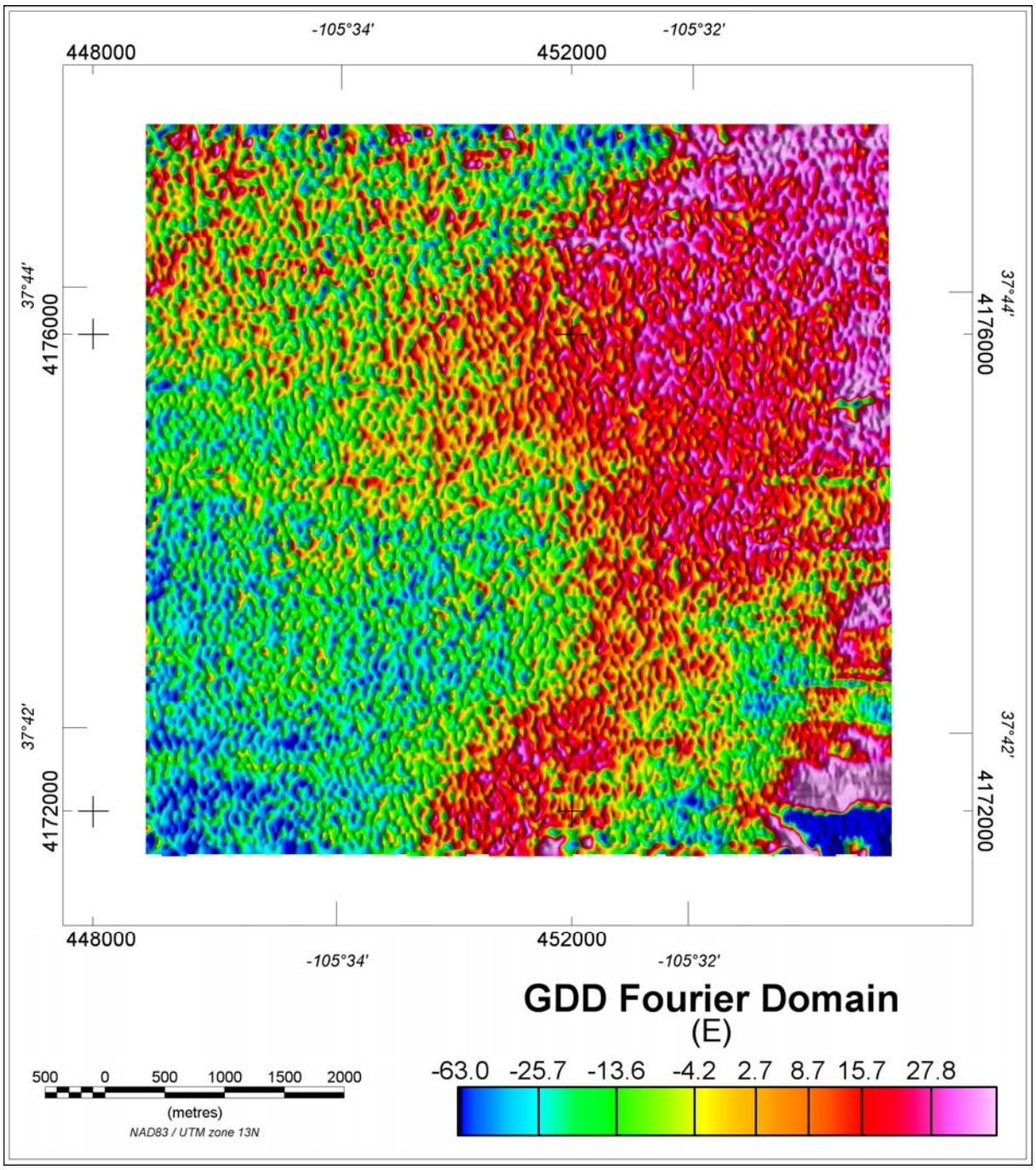

Figure 16: Block 2 – *Vertical Gravity Gradient (G_{DD}) from Fourier processing (E).*

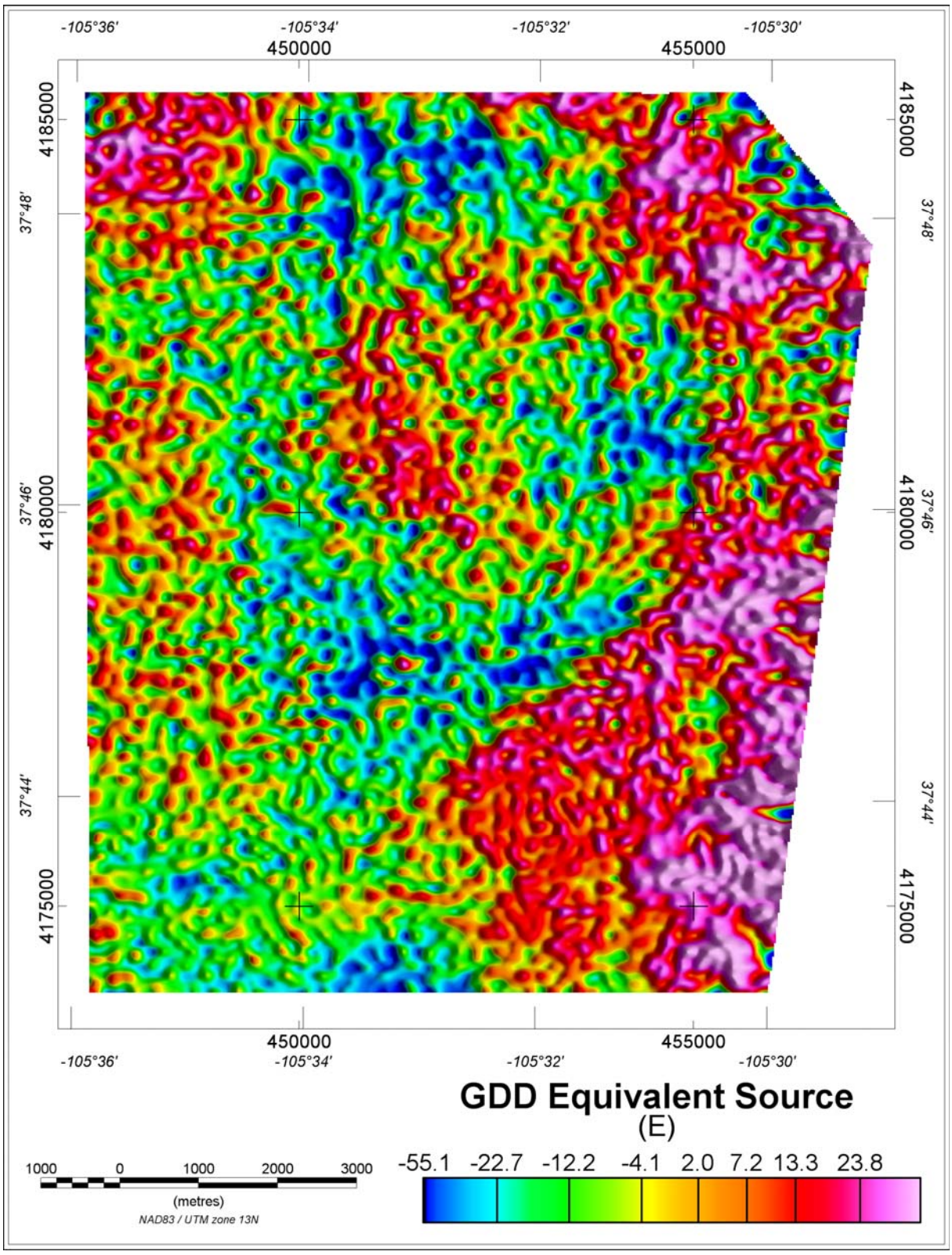

Figure 17: Block 1 – *Vertical Gravity Gradient (G_{DD}) from equivalent source processing (E).*

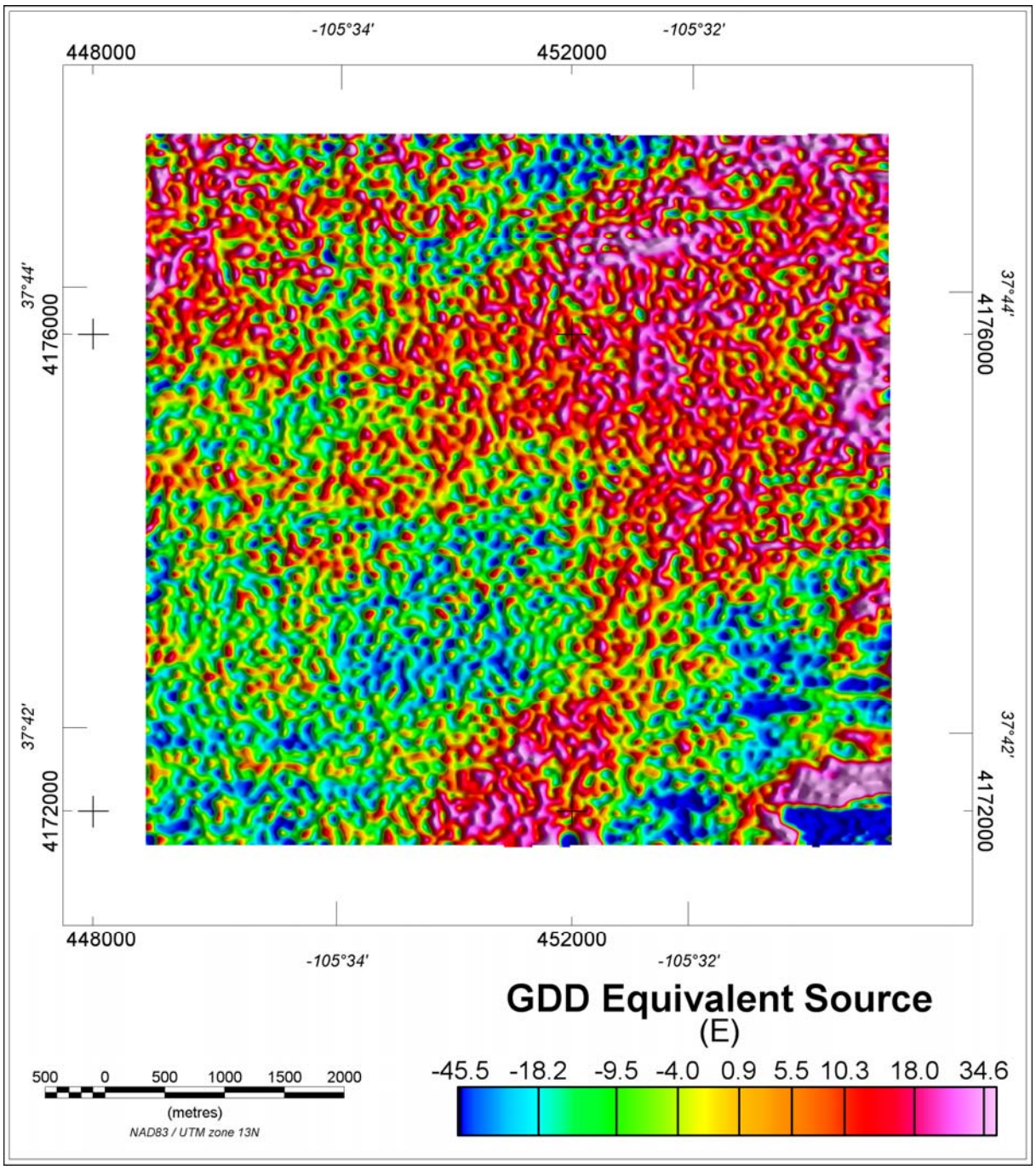

Figure 18: Block 2 – *Vertical Gravity Gradient (G_{DD}) from equivalent source processing (E).*

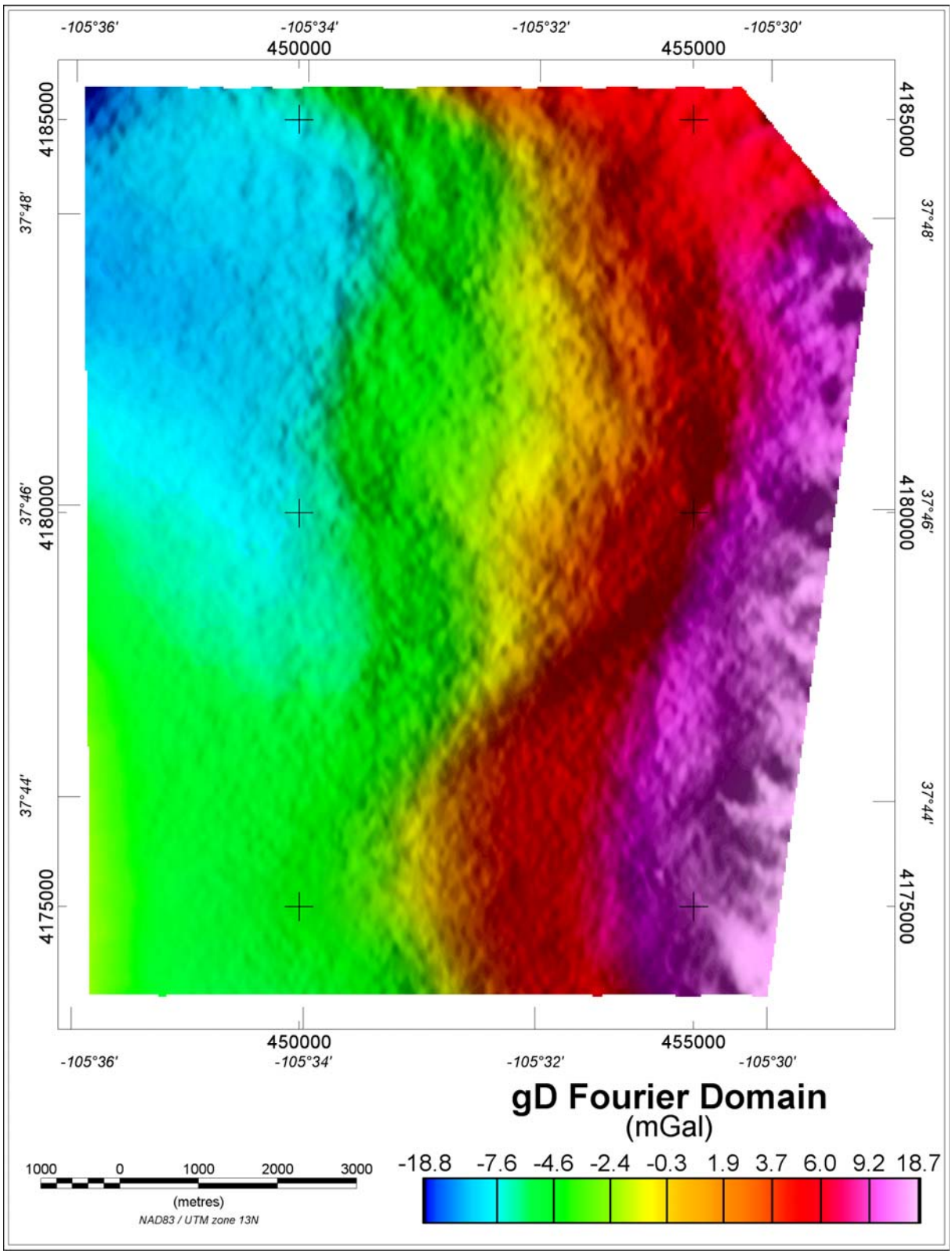

Figure 19: Block 1 – *Vertical Gravity (g_D) from Fourier processing (mGal)*

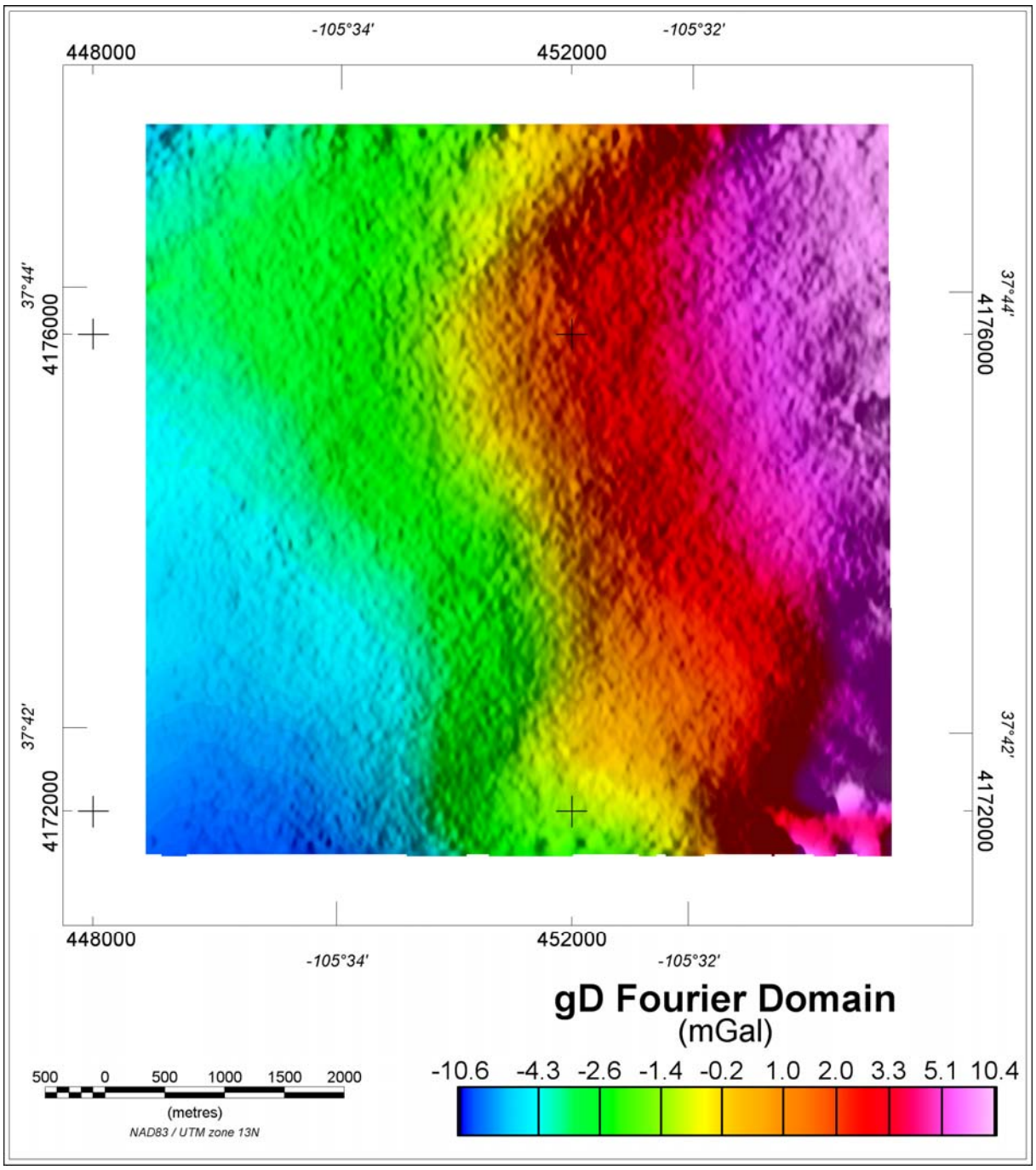

Figure 20: Block 2– *Vertical Gravity (g_D) from Fourier processing (mGal)*

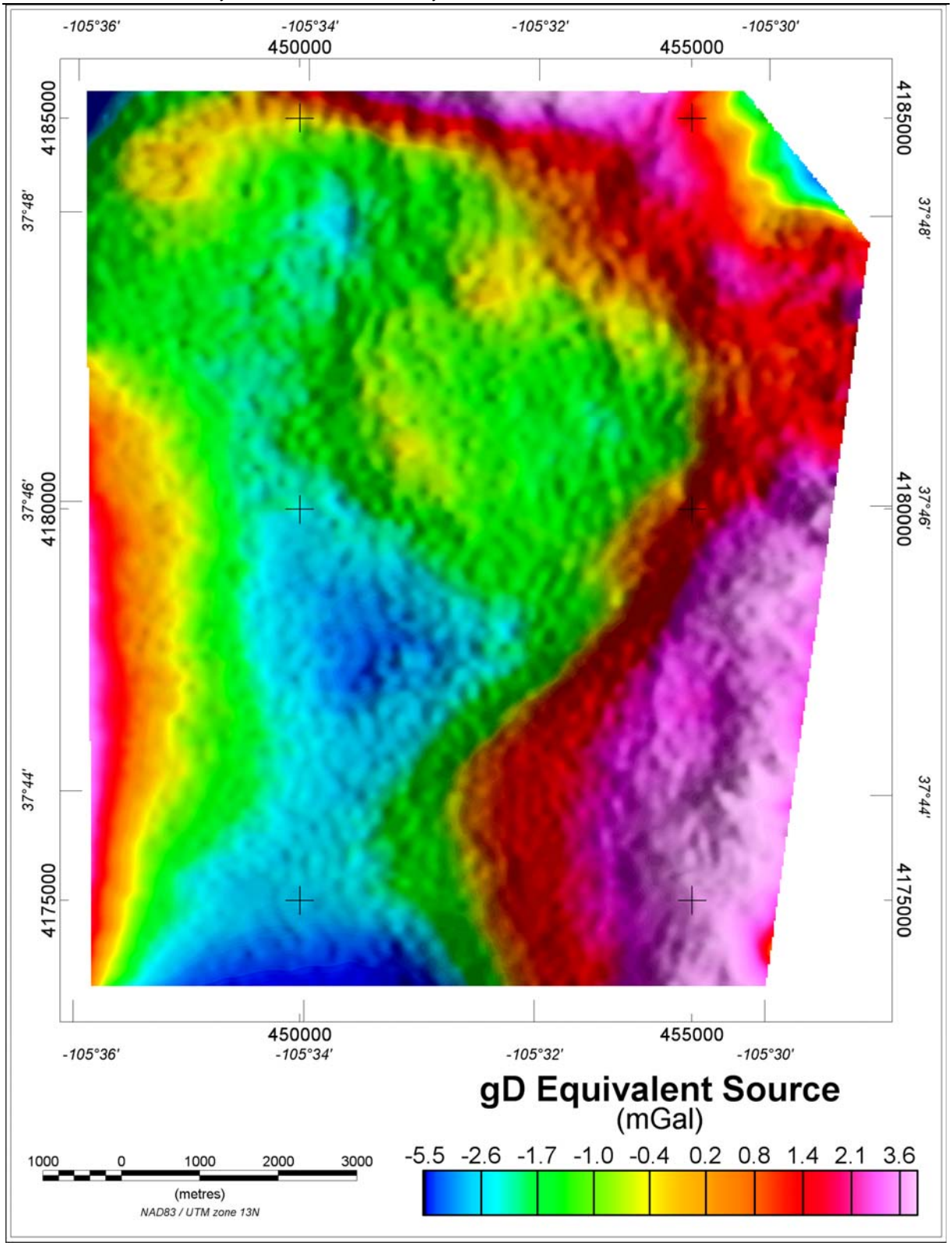

Figure 21: Block 1 – *Vertical Gravity (g_D) from equivalent source processing (mGal)*

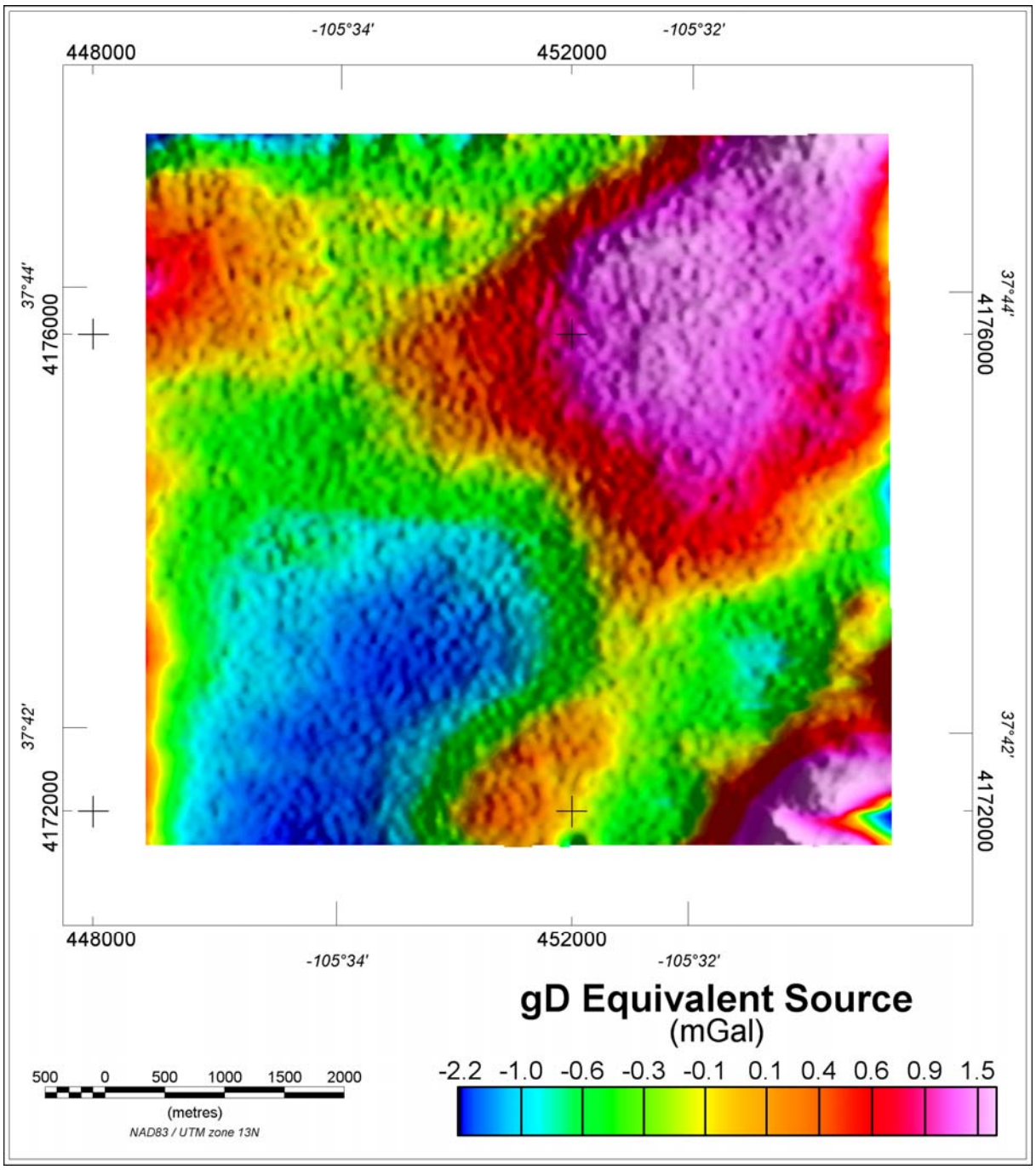

Figure 22: Block 2 – *Vertical Gravity (g_D) from equivalent source processing (mGal)*

5.8 Conforming g_D to regional gravity

As discussed in section 8.3, the long wavelength information in g_D (both the Fourier and equivalent source versions) can be improved by incorporating ancillary information. Such information was provided by the USGS in the form of a regional gravity grid.

The Fourier and equivalent source g_D grids were conformed to the regional grid as follows. The (density 2 g/cm^3) results are presented in *Figure 23*, *Figure 24*, *Figure 25* and *Figure 26.*

- Low pass filter the regional data using a cosine squared filter with cut-off at 15km, tapering to 10km.
- High pass filter the g_D data (Fourier and equivalent source) using a cosine squared filter with cut-off at 15 km, tapering to 10km.
- Conform the Fourier and equivalent source data to the regional data by addition of the filtered grids. The filter design is such that this method provides uniform frequency response across the overlap frequencies.

Further discussion of this method can be found in Dransfield (2010).

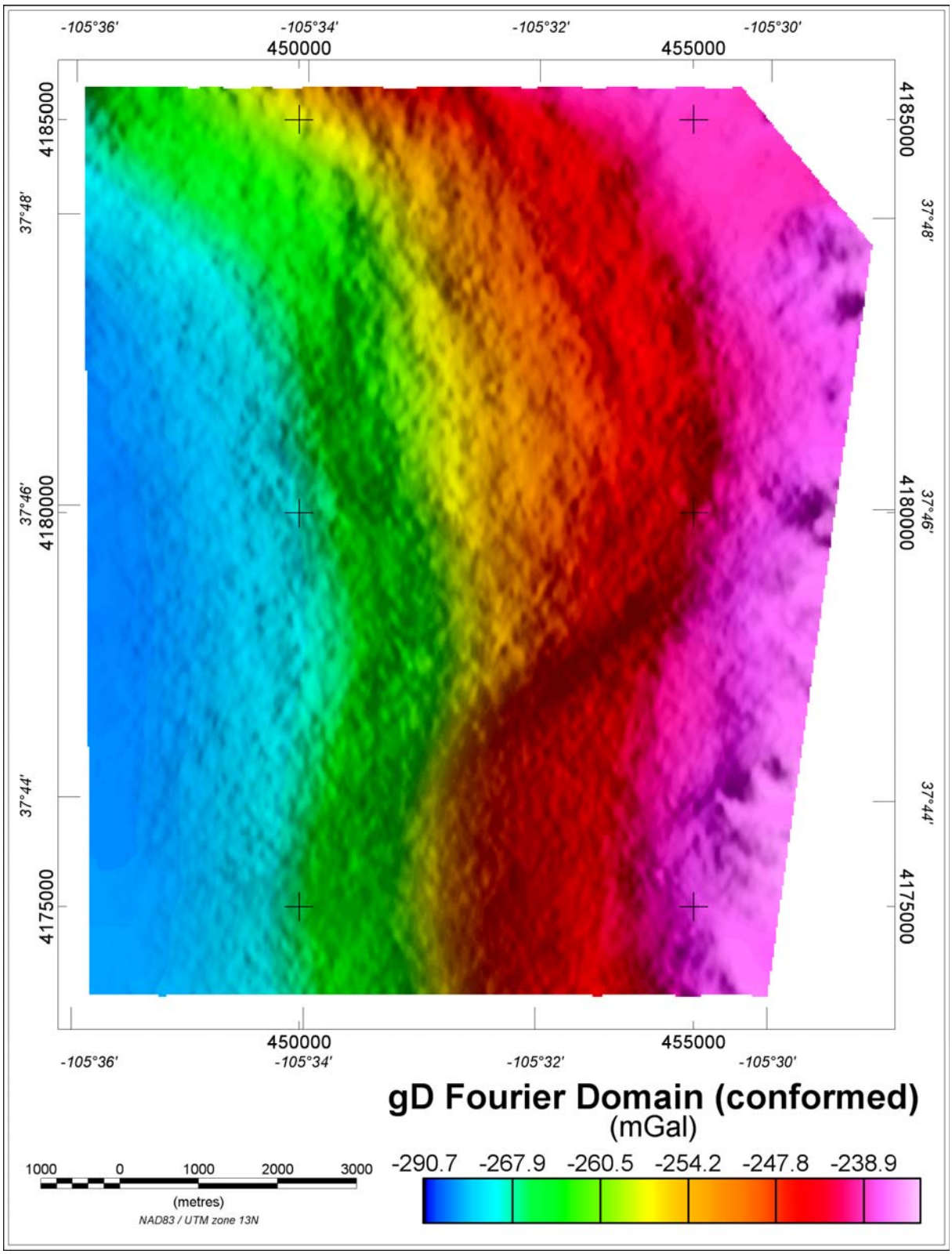

Figure 23: Block 1 – *Vertical Gravity (g_D) from Fourier processing conformed to regional gravity data (mGal)*

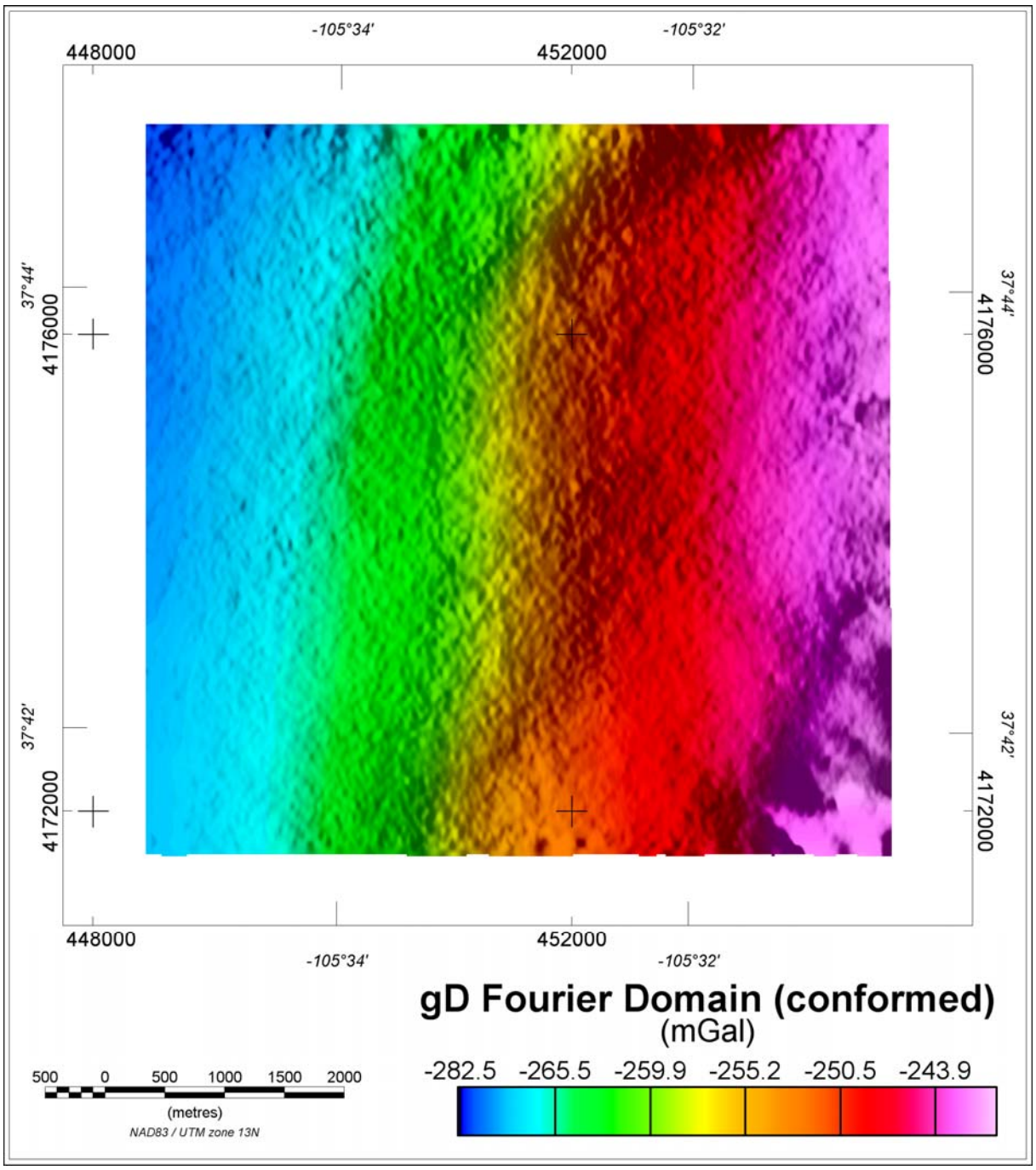

Figure 24: Block 2 – *Vertical Gravity (g_D) from Fourier processing conformed to regional gravity data (mGal)*

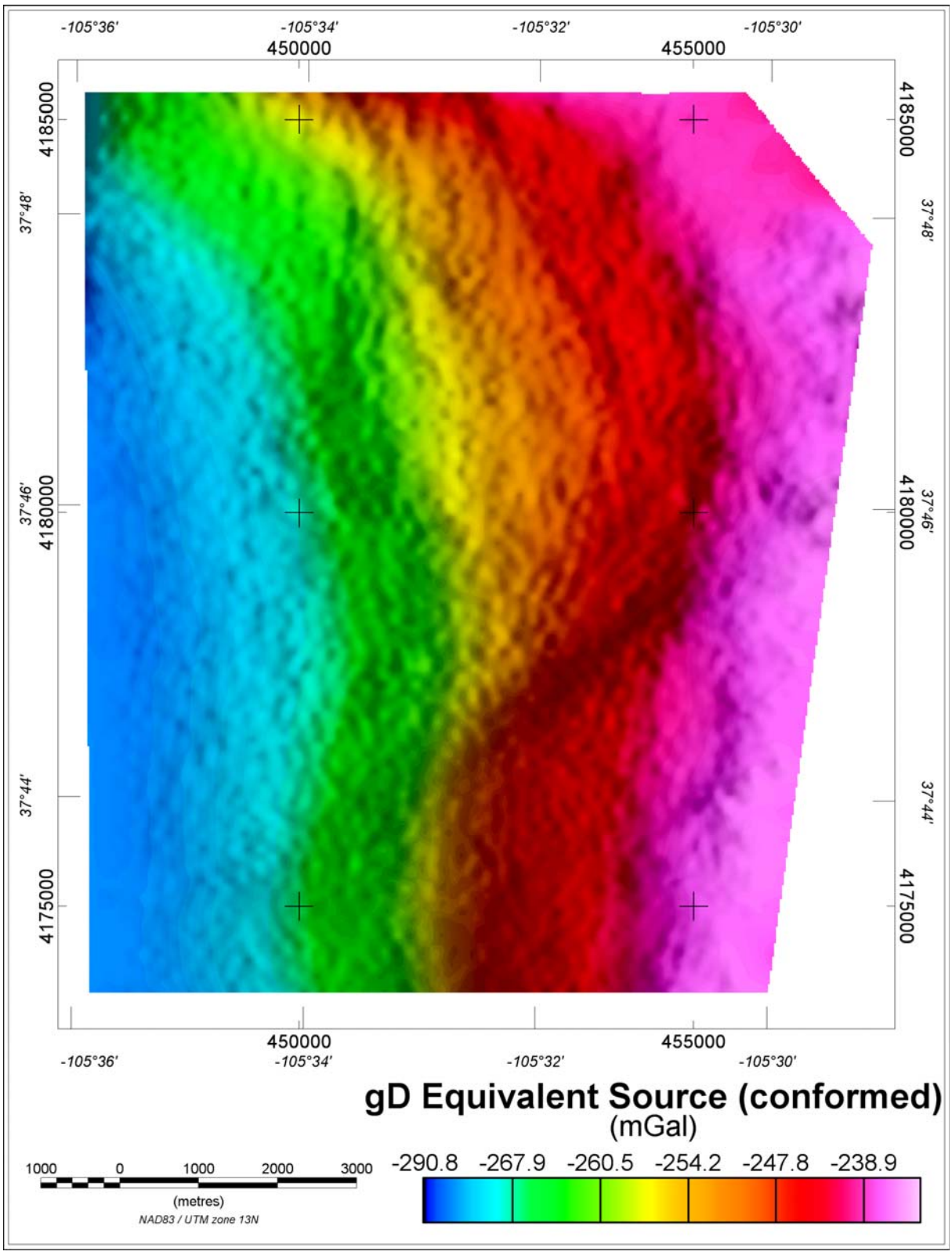

Figure 25: Block 1 – *Vertical Gravity (g_D) from equivalent source processing conformed to regional gravity data (mGal).*

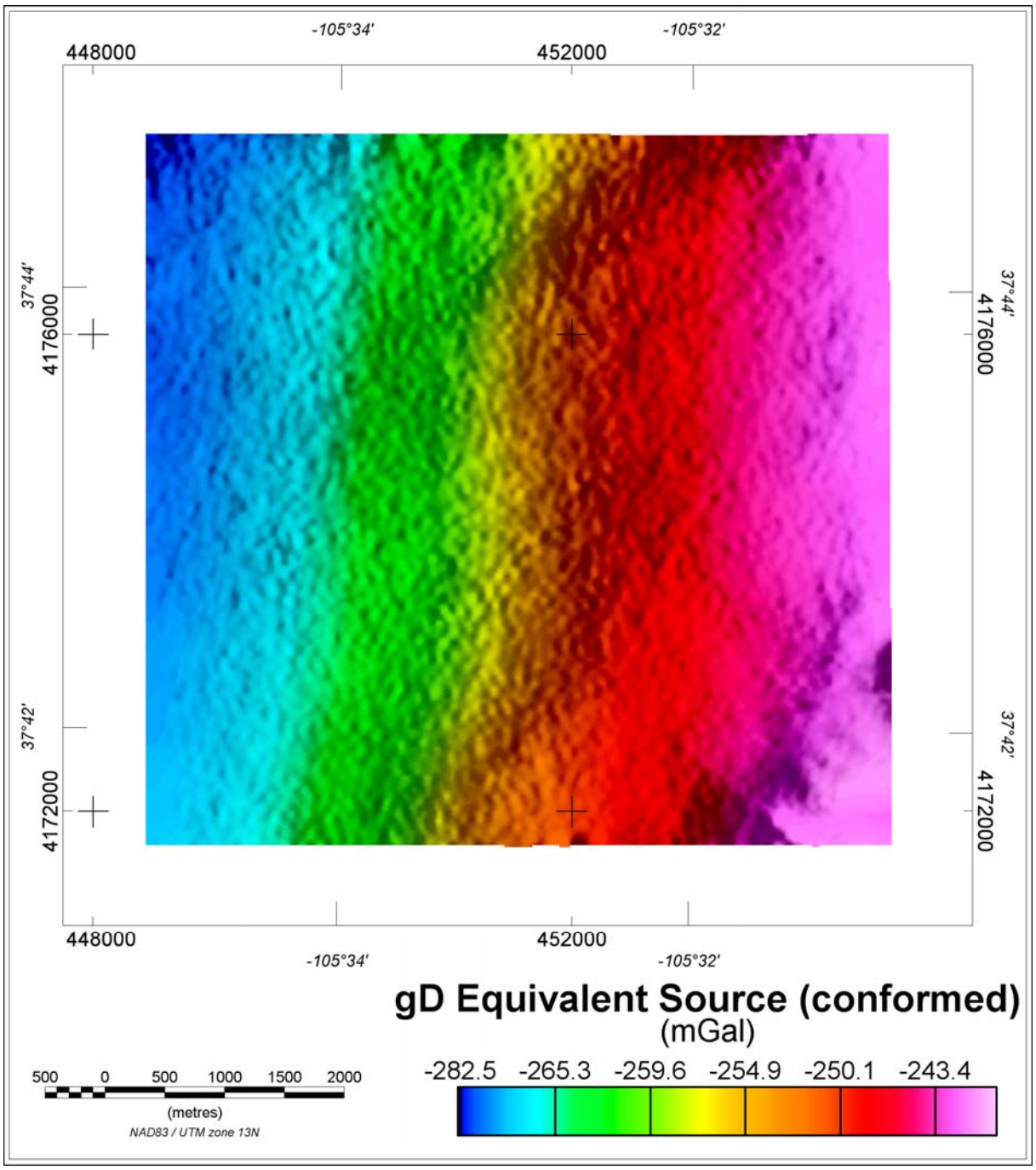

Figure 26: Block 2 – *Vertical Gravity (g_D) from equivalent source processing conformed to regional gravity data (mGal).*

6 APPENDIX I - SURVEY EQUIPMENT

6.1 Survey Aircraft

A Great Slave Helicopters owned Eurocopter AS350-B3 with Canadian registration C-GYAV, was used to fly the survey area. The following instrumentation was used for this survey.

6.2 HeliFALCON™ Airborne Gravity Gradiometer

HeliFALCON™ *AGG System*
The **HeliFALCON**™ AGG System is based on current state-of-the-art airborne gravity gradiometer technology and has been optimized for airborne broad band geophysical exploration. The system is capable of supporting surveying activities in areas ranging from 1,000 ft below sea level to 13,000 ft above sea level with aircraft speeds from 70 to 130 knots. The **HeliFALCON**™ AGG data streams were digitally recorded at different rates on removable drives installed in the **HeliFALCON**™ AGG electronics rack.

6.3 Airborne Data Acquisition Systems

Fugro Digital Acquisition System (FASDAS)
The Fugro FASDAS is a data acquisition system executing propriety software for the acquisition and recording of location, magnetic and ancillary data. Data are presented both numerically and graphically in real time on the VGA display providing on-line quality control capability.

The FASDAS is also used for real time navigation. A pre-programmed flight plan containing boundary coordinates, line start and end coordinates, the altitude values calculated for a theoretical drape surface, line spacing and cross track definitions is loaded into the computer prior to each flight. The WGS-84 latitude and longitude and altitude received from the real-time corrected, dual frequency Novatel OEMV L1/l2-Band Positioning receiver, is transformed to the local coordinate system for cross track and distance to go values. This information, together with ground heading and speed, is displayed to the pilot numerically and graphically on a two line LCD display. It is also presented on the operator LCD screen in conjunction with a pictorial representation of the survey area, survey lines and ongoing flight path.

HeliFALCON™ *AGG Data Acquisition System (ADAS)*
The FASDAS provides control and data display for the **HeliFALCON**™ AGG system. Data is displayed real time for the operator and warnings displayed should system parameters deviate from tolerance specifications. All **HeliFALCON**™ AGG and laser scanner data are recorded to a removable hard drive.

6.4 Real-Time Differential GPS

Novatel OEMV L-Band Positioning
The Novatel OEMV L-band Positioning receiver provides real-time differential GPS for the onboard navigation system. The differential data set was relayed via a geo-synchronous satellite to the aircraft where the receiver optimized the corrections for the current location.

6.5 GPS Base Station Receiver

Novatel OEM4 L1/L2
The Novatel GPS receiver is a 12 channel dual frequency GPS receiver. It provides raw range information of all satellites in view sampled every second and recorded on a computer laptop. These data are post-processed with the rover data to provide differential GPS (DGPS) corrections for the flight path.

6.6 Altimeters

Honeywell RT300 / AT220

6.7 Laser Scanner

Riegl LMS-Q140I-80
The laser scanner is designed for high speed line scanning applications. The system is based upon the principle of time-of-flight measurement of short laser pulses in the infrared wavelength region and the angular deflection of the laser beam is obtained by a rotating polygon mirror wheel. The measurement range is up to 400 m with a minimum range of 2 m and an accuracy of 50mm. The laser beam is eye safe, the laser wavelength is 0.9 μm, the scan angle range is +/- 40° and the scan speed is 20 scans/s.

6.8 Data Processing Hardware and Software

The following equipment and software were used:

Hardware
- One 2.0 GHz (or higher) laptop computer
- External USB hard drive reader for ADAS removable drives
- Two External USB hard drives for data backup
- HP DeskJet All-In-One printer, copier, scanner

Software
- Oasis Montaj data processing and imaging software
- GrafNav Differential GPS processing software
- Fugro - Atlas data processing software
- Fugro - DiAGG processing software

7 APPENDIX II - SYSTEM TESTS

7.1 Instrumentation Lag

Due to the relative position of the magnetometer, altimeters and GPS antenna on the aircraft and to processing/recording time lags, raw readings from each data stream vary in position. To correct for this and to align selected anomaly features on lines flown in opposite directions, the magnetic and altimeter data are 'parallaxed' with respect to the position information. The lags were applied to the data during processing.

7.2 Radar Altimeter Calibration

The radar altimeter is checked for accuracy and linearity every 12 months, or when any change in a key system component requires this procedure to be carried out. This calibration allows the radar altimeter data to be compared and assessed with the other height data (GPS, barometric and laser) to confirm the accuracy of the radar altimeter over its operating range. The calibration is performed by flying a number of 30 second lines at preselected terrain clearances over an area of flat terrain and using the results of the radar altimeter, differentially corrected GPS heights in mean sea level (MSL) and laser scanner were used to derive slope and offset information.

7.3 HeliFALCON™ AGG Noise Measurement

At the commencement of the survey, 20 minutes of data were collected with the aircraft in straight level flight at 3500 ft AGL. These data were processed as a survey line to check the AGG noise levels.

Daily flight debriefs incorporating HeliFALCON™ AGG performance statistics for each flight line are prepared using output from Fugro DiAGG software. These are sent daily to Fugro office staff for performance evaluation.

7.4 Daily Calibrations

A set of daily calibrations were performed each survey day as follows:
AGG Quiescent Calibration

7.4.1 HeliFALCON™ AGG Calibration

A calibration was performed at the beginning of each flight and the results monitored by the operator. The coefficients obtained from each of the calibrations were used in the processing of the data.

8 APPENDIX III - HeliFALCON™ AGG DATA & PROCESSING

8.1 Nomenclature

The **HeliFALCON™** airborne gravity gradiometer (AGG) system adopts a North, East, and Down coordinate sign convention and these directions (N, E, and D) are used as subscripts to identify the gravity gradient tensor components (gravity vector derivatives). Lower case is used to identify the components of the gravity field and upper case to identify the gravity gradient tensor components. Thus the parameter usually measured in a normal exploration ground gravity survey is $\mathbf{g_D}$ and the vertical gradient of this component is $\mathbf{G_{DD}}$.

8.2 Units

The vertical component of gravity ($\mathbf{g_D}$) is delivered in the usual units of mGal. The gradient tensor components are delivered in eotvos, which is usually abbreviated to "E". By definition **1 E = 10^{-4} mGal/m.**

8.3 HeliFALCON™ Airborne Gravity Gradiometer Surveys

In standard ground gravity surveys, the component measured is "$\mathbf{g_D}$", which is the *vertical component of the acceleration due to gravity*. In airborne gravity systems, since the aircraft is itself accelerating, measurement of "$\mathbf{g_D}$" cannot be made to the same precision and accuracy as on the ground. Airborne gravity gradiometry uses a differential measurement to remove the aircraft motion effects and delivers gravity data of a spatial resolution and sensitivity comparable with ground gravity data.

The **HeliFALCON™** gradiometer instrument acquires two curvature components of the gravity gradient tensor namely $\mathbf{G_{NE}}$ and $\mathbf{G_{UV}}$ where $\mathbf{G_{UV}} = (\mathbf{G_{EE}} - \mathbf{G_{NN}})/2$. Since these curvature components cannot easily and intuitively be related to the causative geology, they are transformed into the vertical gravity gradient ($\mathbf{G_{DD}}$), and integrated to derive the vertical component of gravity ($\mathbf{g_D}$). Interpreters display, interpret and model both $\mathbf{G_{DD}}$ and $\mathbf{g_D}$. The directly measured $\mathbf{G_{NE}}$ and $\mathbf{G_{UV}}$ data are appropriate for use in inversion software to generate density models of the earth. The vertical gravity gradient, $\mathbf{G_{DD}}$, is more sensitive to small or shallow sources and has greater spatial resolution than $\mathbf{g_D}$ (similar to the way that the vertical magnetic gradient provides greater spatial resolution and increased sensitivity to shallow sources of the magnetic field). In the integration of $\mathbf{G_{DD}}$ to give $\mathbf{g_D}$, the very long wavelength component, at wavelengths comparable to or greater than the size of the survey area, cannot be fully recovered. Long wavelength gravity are therefore incorporated in the $\mathbf{g_D}$ data from other sources. This might be regional ground, airborne or marine gravity if such data are available. The Danish National Space Centre global gravity data of 2008 (DNSC08) are used as a default if other data are not available.

8.4 Gravity Data Processing

The main elements and sequence of processing of the gravity data are as follows:

1. Dynamic corrections for residual aircraft motion (called Post Mission Compensation or PMC) are calculated and applied.
2. Self gradient corrections are calculated and applied to reduce the time-varying gradient response from the aircraft and platform.
3. A Digital Terrain Model (DTM) is created from the laser scanner range data, the AGG inertial navigation system rotation data and the DGPS position data.
4. Terrain corrections are calculated and applied.

5. $\mathbf{G_{NE}}$ and $\mathbf{G_{UV}}$ are levelled and transformed into the full gravity gradient tensor, including $\mathbf{G_{DD}}$, and into $\mathbf{g_D}$.

8.5 Aircraft dynamic corrections

The design and operation of the **HeliFALCON™** AGG results in very considerable reduction of the effects of aircraft acceleration but residual levels are still significant and further reduction is required and must be done in post-processing.

Post-processing correction relies on monitoring the inertial acceleration environment of the gravity gradiometer instrument (GGI) and constructing a model of the response of the GGI to this environment. Parameters of the model are adjusted by regression to match the sensitivity of the GGI during data acquisition. The modelled GGI output in response to the inertial sensitivities is subtracted from the observed output. Application of this technique to the output of the GGI, when it is adequately compensated by its internal mechanisms, reduces the effect of aircraft motion to acceptable levels.

Following these corrections, the gradient data are demodulated and filtered along line with a 6-pole Butterworth low-pass filter with a cut-off frequency of 0.18 Hz (for fixed-wing operations; a higher frequency may be used for helicopter operations).

8.6 Self gradient Corrections

The GGI is mounted in gimbals controlled by an inertial navigation system which keeps the GGI pointing in a fixed direction whilst the aircraft and gimbals rotate around it. Consequently, the GGI measures a time-varying gravity gradient due to these masses moving around it as the heading and attitude of the aircraft changes during flight. This is called the self-gradient.

Like the aircraft dynamic corrections, the self-gradient is calculated by regression of model parameters against measured data. In this case, the rotations of the gimbals are the input variables of the model. Once calculated, the modelled output is subtracted from the observed output.

8.7 Laser Scanner Processing

The laser scanner measures the range from the aircraft to the ground in a swathe of angular width ±40 degrees below the aircraft. The aircraft attitude (roll, pitch and heading) data provided by the AGG inertial navigation system are used to adjust the range data for changes in attitude and the processed differential GPS data are used to reference the range data to located ground elevations referenced to the WGS 84 datum. Statistical filtering strategies are used to remove anomalous elevations due to foliage or built up environment. The resulting elevations are gridded to form a digital terrain model (DTM).

8.8 Terrain Corrections

An observation point above a hill has excess mass beneath it compared to an observation point above a valley. Since gravity is directly proportional to the product of the masses, uncorrected gravity data have a high correlation with topography.

It is therefore necessary to apply a terrain correction to gravity survey data. For airborne gravity gradiometry at low survey heights, a detailed DTM is required. Typically, immediately below the aircraft, the digital terrain will need to be sampled at a cell size

roughly one-third to one-half of the survey height and with a position accuracy of better than 1 metre. For these accuracies, LIDAR data are required and each **HeliFALCON™** survey aircraft comes equipped with LIDAR (laser scanner).

If bathymetric data are used then these form a separate terrain model for which terrain corrections are calculated at a density chosen to suit the water bottom – water interface. Once the DTM has been merged, the terrain corrections for each of the $\mathbf{G_{NE}}$ and $\mathbf{G_{UV}}$ data streams are calculated. In the calculation of terrain corrections, a density of 1 gm/cc is used. The calculated corrections are stored in the database allowing the use of any desired terrain correction density by subtracting the product of desired density and correction from the measured $\mathbf{G_{NE}}$ and $\mathbf{G_{UV}}$ data. The terrain correction density is chosen to be representative of the terrain density over the survey area. Sometimes more than one density is used with input from the client.

Typically, the terrain corrections are calculated over a distance 10 km from each survey measurement point.

8.9 Tie-line Levelling

The terrain- and Self gradient-corrected $\mathbf{G_{NE}}$ and $\mathbf{G_{UV}}$ data are tie-line levelled across the entire survey using a least-squares minimisation of differences at survey line intersections. Occasionally some micro-levelling might be performed.

8.10 Transformation into G_{DD} & g_D

The transformation of the measured, corrected and levelled $\mathbf{G_{NE}}$ and $\mathbf{G_{UV}}$ data into gravity and components of the full gravity gradient tensor is accomplished using two methods:

- Fourier domain transformation and
- Equivalent source transformation.

The Fourier method relies on the Fourier transform of Laplace's equation. The application of this transform to the complex function $\mathbf{G_{NE} + i\, G_{UV}}$ provides a stable and accurate calculation of each of the full tensor components and gravity. The Fourier method performs piece-wise upward and downward continuation to work with data collected on a surface that varies from a flat horizontal plane. For stability of the downward continuation, the data are low-pass filtered. The cut-off wavelength of this filter depends on the variations in altitude and the line spacing. It is set to the smallest value that provides stable downward continuation.

The equivalent source method relies on a smooth model inversion to calculate the density of a surface of sources and from these sources, a forward calculation provides the $\mathbf{G_{DD}}$ and $\mathbf{g_D}$ data. The smoothing results in an output that is equivalent to the result of the low-pass filter in the Fourier domain method.

The Fourier method generates all tensor components but the equivalent source method only generates $\mathbf{G_{DD}}$ and $\mathbf{g_D}$ (and $\mathbf{G_{NE}}$ and $\mathbf{G_{UV}}$ for comparison with the inputs).

The limitations of gravity gradiometry in reconstructing the long wavelengths of gravity can lead to differences in the results of these two methods at long wavelength. The merging of the $\mathbf{g_D}$ data with externally supplied regional gravity such as the DNSC08 gravity removes these differences.

8.11 Noise & Signal

With all the **HeliFALCON™** AGG instruments, there are two measurements made of both the NE and UV curvature components during acquisition. This gives a pair of independent readings at each sample point.

The standard deviation of half the difference between these pairs is a good estimate of the survey noise. This is calculated for each line, and the average of all the survey lines is the figure quoted for the survey as a whole.

This difference error has been demonstrated to follow a 'normal' or Gaussian statistical distribution, with a mean of zero. Therefore, the bulk of the population (95%) will lie between -2σ and +2σ of the mean. For a typical survey noise estimate of, say, 3 E, 95% of the noise will be between -6 E and +6 E.

These typical errors in the curvature gradients translate to errors in $\mathbf{G_{DD}}$ of about 5 E and in $\mathbf{g_D}$ (in the shorter wavelengths) in the order of 0.1 mGal.

8.12 Risk Criteria in Interpretation

The risks associated with a **HeliFALCON™** AGG survey are mainly controlled by the following factors.

- **Survey edge anomalies** – the transformation from measured curvature gradients to vertical gradient and vertical gravity gradient is subject to edge effects. Hence any anomalies located within about 2 x line spacing of the edge of the survey boundaries should be treated with caution.
- **Single line anomalies** – for a wide-spaced survey, an anomaly may be present on only one line. Although it might be a genuine anomaly, the interpreter should note that no two-dimensional control can be applied.
- **Low amplitude (less than 2σ) anomalies** – Are within the noise envelope and need to be treated with caution, if they are single line anomalies and close in diameter to the cut-off wavelengths used.
- **Residual topographic error anomalies** – Inaccurate topographic correction either due to inaccurate DTM or local terrain density variations may produce anomalies. Comparing the DTM with the G_{DD} map terrain-corrected for different densities is a reliable way to confirm the legitimacy of an anomaly.
- **The low density of water and lake sediments** – (if present) can create significant gravity and gravity gradient lows which may be unrelated to bedrock geology. It is recommended that all anomalies located within lakes or under water be treated with caution and assessed with bathymetry if available.

8.13 References

Boggs, D. B. and Dransfield, M. H., 2004, Analysis of errors in gravity derived from the Falcon airborne gravity gradiometer, Lane, R. (ed.), Airborne Gravity 2004 - Abstracts from the ASEG-PESA Airborne Gravity 2004 Workshop, Geoscience Australia Record 2004/18, 135-141.

Dransfield, M. H., 2010, Conforming Falcon gravity and the global gravity anomaly, Geophysical Prospecting, 58, 469-483.

Dransfield, M. H. and Lee, J. B., 2004, The FALCON airborne gravity gradiometer survey systems, Lane, R. (ed.), Airborne Gravity 2004 - Abstracts from the ASEG-PESA Airborne Gravity 2004 Workshop, Geoscience Australia Record 2004/18, 15-19.

Dransfield, M. H. and Zeng, Y., Airborne gravity gradiometry: terrain corrections and elevation error, *submitted to Geophysics*.

Lee, J. B., 2001, FALCON Gravity Gradiometer Technology, Exploration Geophysics, 32, 75-79.

Lee, J. B.; Liu, G.; Rose, M.; Dransfield, M.; Mahanta, A.; Christensen, A. and Stone, P., 2001, High resolution gravity surveys from a fixed wing aircraft, Geoscience and Remote Sensing Symposium, 2001. IGARSS '01. IEEE 2001 International, 3, 1327-1331.

Stone, P. M. and Simsky, A., 2001, Constructing high resolution DEMs from Airborne Laser Scanner Data, Preview, Extended Abstracts: ASEG 15th Geophysical Conference and Exhibition, August 2001, Brisbane, 93, 99.

9 APPENDIX IV - FINAL PRODUCTS

For each area, final **HeliFALCON™** AGG digital line data were provided in 8 Hz Geosoft Oasis GDB database files containing the fields and format described in *Table 3* below. In the Block 2 database there are no Fourier derived channels continued to the smoothed drape surface.

For each area, grids of Fourier and equivalent source products as well as the DTM were delivered, as described in *Table 4* below. The grids are in Geosoft GRD format with a 25 m cell size for Block 1 grids and a 12.5 m grid cell size for block 2 grids with the exception of the DTM grids which have a 10 m cell size. For Block 2, there are no Fourier derived grids continued to the smoothed drape surface.

Two copies of the digital archives were delivered along with a hard copy of this Logistics and Processing Report.

Field	Variable	Description	Units
1	Line	Line number	
2	Flight	Flight number	
3	x_nad83	NAD83 UTM13N Easting	metres
4	y_nad83	NAD83 UTM13N Northing	metres
5	long_nad83	NAD83 Longitude	degrees
6	lat_nad83	NAD83 Latitude	degrees
7	ALTITUDE_Ellipsoid	Height above NAD83 ellipsoid	metres
8	ALTITUDE	GPS sensor height above WGS84 ellipsoid with geoid (EGM96) correction applied	metres
9	time	Universal Time (seconds since January 6 1980)	seconds
10	height	Flying height (aircraft's height above terrain as derived from laser scanner and ALTITUDE data)	metres
11	DTM	Terrain height above WGS84 ellipsoid with Geoid (EGM96) correction applied	metres
12	TURBULENCE	Estimated vertical platform turbulence (vertical acceleration where g = 9.80665 m/sec/sec)	milli g
13	T_DD	Terrain effect calculated for DD using a density of 1g/cc	eotvos
14	T_NE	Terrain effect calculated for NE using a density of 1g/cc	eotvos
15	T_UV	Terrain effect calculated for UV using a density of 1g/cc	eotvos
16	Err_NE	NE gradient uncorrelated noise estimate, after levelling	eotvos
17	Err_UV	UV gradient uncorrelated noise estimate, after levelling	eotvos
18	A_NE_2p67	Self gradient, jitter & terrain corrected NE gradient, terrain correction density 2.67 g/cc	eotvos
19	A_UV_2p67	Self gradient, jitter & terrain corrected UV gradient, terrain correction density 2.67 g/cc	eotvos
20	B_NE_2p67	Self gradient, jitter & terrain corrected NE gradient, terrain correction density 2.67 g/cc	eotvos
21	B_UV_2p67	Self gradient, jitter & terrain corrected UV gradient, terrain correction density 2.67 g/cc	eotvos
22	A_NE_2	Self gradient, jitter & terrain corrected NE gradient, terrain correction density 2 g/cc	eotvos
23	A_UV_2	Self gradient, jitter & terrain corrected UV gradient, terrain correction density 2 g/cc	eotvos
24	B_NE_2	Self gradient, jitter & terrain corrected NE gradient, terrain correction density 2 g/cc	eotvos

25	B_UV_2	Self gradient, jitter & terrain corrected UV gradient, terrain correction density 2 g/cc	eotvos
26	A_NE_0	Self gradient & jitter corrected NE gradient, no terrain correction applied	eotvos
27	A_UV_0	Self gradient & jitter corrected UV gradient, no terrain correction applied	eotvos
28	B_NE_0	Self gradient & jitter corrected NE gradient, no terrain correction applied	eotvos
29	B_UV_0	Self gradient & jitter corrected UV gradient, no terrain correction applied	eotvos
30	gD_FOURIER_2p67_100_NC	Fourier derived vertical Gravity, terrain correction density 2.67 g/cc, 100 m cut-off wavelength, no continuation	mGal
31	GDD_FOURIER_2p67_100_NC	Fourier derived vertical gravity gradient, terrain correction density 2.67 g/cc, 100 m cut-off wavelength, no continuation	eotvos
32	GEE_FOURIER_2p67_100_NC	Fourier derived Gee gradient, terrain correction density 2.67 g/cc, 100 m cut-off wavelength, no continuation	eotvos
33	GNN_FOURIER_2p67_100_NC	Fourier derived Gnn gradient, terrain correction density 2.67 g/cc, 100 m cut-off wavelength, no continuation	eotvos
34	GED_FOURIER_2p67_100_NC	Fourier derived Ged horizontal EW gradient, terrain correction density 2.67 g/cc, 100 m cut-off wavelength, no continuation	eotvos
35	GND_FOURIER_2p67_100_NC	Fourier derived Gnd horizontal NS gradient, terrain correction density 2.67 g/cc, 100 m cut-off wavelength, no continuation	eotvos
36	GNE_FOURIER_2p67_100_NC	Fourier derived Gne curvature gradient, terrain correction density 2.67 g/cc, 100 m cut-off wavelength, no continuation	eotvos
37	GUV_FOURIER_2p67_100_NC	Fourier derived Guv curvature gradient, terrain correction density 2.67 g/cc, 100 m cut-off wavelength, no continuation	eotvos
38	gD_FOURIER_2_100_NC	Fourier derived vertical Gravity, terrain correction density 2 g/cc, 100 m cut-off wavelength, no continuation	mGal
39	GDD_FOURIER_2_100_NC	Fourier derived vertical gravity gradient, terrain correction density 2 g/cc, 100 m cut-off wavelength, no continuation	eotvos
40	GEE_FOURIER_2_100_NC	Fourier derived Gee gradient, terrain correction density 2 g/cc, 100 m cut-off wavelength, no continuation	eotvos
41	GNN_FOURIER_2_100_NC	Fourier derived Gnn gradient, terrain correction density 2 g/cc, 100 m cut-off wavelength, no continuation	eotvos
42	GED_FOURIER_2_100_NC	Fourier derived Ged horizontal EW gradient, terrain correction density 2 g/cc, 100 m cut-off wavelength, no continuation	eotvos
43	GND_FOURIER_2_100_NC	Fourier derived Gnd horizontal NS gradient, terrain correction density 2 g/cc, 100 m cut-off wavelength, no continuation	eotvos
44	GNE_FOURIER_2_100_NC	Fourier derived Gne curvature gradient, terrain correction density 2 g/cc, 100 m cut-off wavelength, no continuation	eotvos
45	GUV_FOURIER_2_100_NC	Fourier derived Guv curvature gradient, terrain correction density 2 g/cc, 100 m cut-off wavelength, no continuation	eotvos
46	gD_FOURIER_0_100_NC	Fourier derived vertical Gravity, no terrain correction applied, 100 m cut-off wavelength, no continuation	mGal
47	GDD_FOURIER_0_100_NC	Fourier derived vertical gravity gradient, no terrain correction applied, 100 m cut-off wavelength, no continuation	eotvos
48	GEE_FOURIER_0_100_NC	Fourier derived Gee gradient, no terrain correction applied, 100 m cut-off wavelength, no continuation	eotvos
49	GNN_FOURIER_0_100_NC	Fourier derived Gnn gradient, no terrain correction applied, 100 m cut-off wavelength, no continuation	eotvos
50	GED_FOURIER_0_100_NC	Fourier derived Ged horizontal EW gradient, no terrain correction applied, 100 m cut-off wavelength, no continuation	eotvos
51	GND_FOURIER_0_100_NC	Fourier derived Gnd horizontal NS gradient, no terrain correction applied, 100 m cut-off wavelength, no continuation	eotvos
52	GNE_FOURIER_0_100_NC	Fourier derived Gne curvature gradient, no terrain correction applied, 100 m cut-off wavelength, no continuation	eotvos
53	GUV_FOURIER_0_100_NC	Fourier derived Guv curvature gradient, no terrain correction applied, 100 m cut-off wavelength, no continuation	eotvos

54	UNSMOOTHED_DRAPESURFACE_FOURIER	Drape surface for Fourier reconstruction, unsmoothed flight surface	metres
55	gD_FOURIER_2p67_300_C	Fourier derived vertical Gravity, terrain correction density 2.67 g/cc, 300 m cut-off wavelength, with continuation	mGal
56	GDD_FOURIER_2p67_300_C	Fourier derived vertical gravity gradient, terrain correction density 2.67 g/cc, 300 m cut-off wavelength, with continuation	eotvos
57	GEE_FOURIER_2p67_300_C	Fourier derived Gee gradient, terrain correction density 2.67 g/cc, 300 m cut-off wavelength, with continuation	eotvos
58	GNN_FOURIER_2p67_300_C	Fourier derived Gnn gradient, terrain correction density 2.67 g/cc, 300 m cut-off wavelength, with continuation	eotvos
59	GED_FOURIER_2p67_300_C	Fourier derived Ged horizontal EW gradient, terrain correction density 2.67 g/cc, 300 m cut-off wavelength, with continuation	eotvos
60	GND_FOURIER_2p67_300_C	Fourier derived Gnd horizontal NS gradient, terrain correction density 2.67 g/cc, 300 m cut-off wavelength, with continuation	eotvos
61	GNE_FOURIER_2p67_300_C	Fourier derived Gne curvature gradient, terrain correction density 2.67 g/cc, 300 m cut-off wavelength, with continuation	eotvos
62	GUV_FOURIER_2p67_300_C	Fourier derived Guv curvature gradient, terrain correction density 2.67 g/cc, 300 m cut-off wavelength, with continuation	eotvos
63	gD_FOURIER_2_300_C	Fourier derived vertical Gravity, terrain correction density 2 g/cc, 300 m cut-off wavelength, with continuation	mGal
64	GDD_FOURIER_2_300_C	Fourier derived vertical gravity gradient, terrain correction density 2 g/cc, 300 m cut-off wavelength, with continuation	eotvos
65	GEE_FOURIER_2_300_C	Fourier derived Gee gradient, terrain correction density 2 g/cc, 300 m cut-off wavelength, with continuation	eotvos
66	GNN_FOURIER_2_300_C	Fourier derived Gnn gradient, terrain correction density 2 g/cc, 300 m cut-off wavelength, with continuation	eotvos
67	GED_FOURIER_2_300_C	Fourier derived Ged horizontal EW gradient, terrain correction density 2 g/cc, 300 m cut-off wavelength, with continuation	eotvos
68	GND_FOURIER_2_300_C	Fourier derived Gnd horizontal NS gradient, terrain correction density 2 g/cc, 300 m cut-off wavelength, with continuation	eotvos
69	GNE_FOURIER_2_300_C	Fourier derived Gne curvature gradient, terrain correction density 2 g/cc, 300 m cut-off wavelength, with continuation	eotvos
70	GUV_FOURIER_2_300_C	Fourier derived Guv curvature gradient, terrain correction density 2 g/cc, 300 m cut-off wavelength, with continuation	eotvos
71	gD_FOURIER_0_300_C	Fourier derived vertical Gravity, no terrain correction applied, 300 m cut-off wavelength, with continuation	mGal
72	GDD_FOURIER_0_300_C	Fourier derived vertical gravity gradient, no terrain correction applied, 300 m cut-off wavelength, with continuation	eotvos
73	GEE_FOURIER_0_300_C	Fourier derived Gee gradient, no terrain correction applied, 300 m cut-off wavelength, with continuation	eotvos
74	GNN_FOURIER_0_300_C	Fourier derived Gnn gradient, no terrain correction applied, 300 m cut-off wavelength, with continuation	eotvos
75	GED_FOURIER_0_300_C	Fourier derived Ged horizontal EW gradient, no terrain correction applied, 300 m cut-off wavelength, with continuation	eotvos
76	GND_FOURIER_0_300_C	Fourier derived Gnd horizontal NS gradient, no terrain correction applied, 300 m cut-off wavelength, with continuation	eotvos
77	GNE_FOURIER_0_300_C	Fourier derived Gne curvature gradient, no terrain correction applied, 300 m cut-off wavelength, with continuation	eotvos
78	GUV_FOURIER_0_300_C	Fourier derived Guv curvature gradient, no terrain correction applied, 300 m cut-off wavelength, with continuation	eotvos
79	SMOOTHED_DRAPESURFACE_FOURIER	Drape surface for Fourier reconstruction, smoothed flight surface	metres
80	gD_EQUIV_2p67	Equivalent source derived vertical gravity, terrain correction density 2.67 g/cc - source depth 100 m	mGal
81	GDD_EQUIV_2p67	Equivalent source derived vertical gravity gradient, terrain correction density 2.67 g/cc - source depth 100 m	eotvos

82	GNE_EQUIV_2p67	Equivalent source derived Gne curvature gradient, terrain correction density 2.67 g/cc - source depth 100 m	eotvos
83	GUV_EQUIV_2p67	Equivalent source derived Guv curvature gradient, terrain correction density 2.67 g/cc - source depth 100 m	eotvos
84	gD_EQUIV_2	Equivalent source derived vertical gravity, terrain correction density 2 g/cc - source depth 100 m	mGal
85	GDD_EQUIV_2	Equivalent source derived vertical gravity gradient, terrain correction density 2 g/cc - source depth 100 m	eotvos
86	GNE_EQUIV_2	Equivalent source derived Gne curvature gradient, terrain correction density 2 g/cc - source depth 100 m	eotvos
87	GUV_EQUIV_2	Equivalent source derived Guv curvature gradient, terrain correction density 2 g/cc - source depth 100 m	eotvos
88	gD_EQUIV_0	Equivalent source derived vertical gravity, no terrain correction applied - source depth 100 m	mGal
89	GDD_EQUIV_0	Equivalent source derived vertical gravity gradient, no terrain correction applied - source depth 100 m	eotvos
90	GNE_EQUIV_0	Equivalent source derived Gne curvature gradient, no terrain correction applied - source depth 100 m	eotvos
91	GUV_EQUIV_0	Equivalent source derived Guv curvature gradient, no terrain correction applied - source depth 100 m	eotvos
92	DRAPESURFACE_EQUIV	Drape surface for equivalent source reconstruction, smoothed flight surface	metres

Table 3: Final HeliFALCON™ AGG Digital Data – *Geosoft Database Format*

File	Description	Units
DTM	Terrain (Referenced to EGM96 Datum)	metres
Equiv_drape_surface	Drape surface for equivalent source construction	metres
Equiv_gD_0	Equivalent source derived vertical gravity, no terrain correction applied	mGal
Equiv_gD_0_conformed	Equivalent source derived vertical gravity, no terrain correction applied, conformed to regional gravity	mGal
Equiv_GDD_0	Equivalent source derived vertical gravity gradient, no terrain correction applied	eotvos
Equiv_sources_0	Plate source surface density, no terrain correction applied	mass per unit area
Equiv_gD_2	Equivalent source derived vertical gravity, terrain correction density 2 g/cm^3	mGal
Equiv_gD_2_conformed	Equivalent source derived vertical gravity, terrain correction density 2 g/cm^3 conformed to regional gravity	mGal
Equiv_GDD_2	Equivalent source derived vertical gravity gradient, terrain correction density 2 g/cm^3	eotvos
Equiv_sources_2	Plate source surface density, terrain correction density 2 g/cm^3	mass per unit area
Equiv_gD_2p67	Equivalent source derived vertical gravity, terrain correction density 2.67 g/cm^3	mGal
Equiv_gD_2p67_conformed	Equivalent source derived vertical gravity, terrain correction density 2.67 g/cm^3 conformed to regional gravity	mGal
Equiv_GDD_2p67	Equivalent source derived vertical gravity gradient, terrain correction density 2.67 g/cm^3	eotvos
Equiv_sources_2p67	Plate source surface density, terrain correction density 2.67 g/cm^3	mass per unit area

Smoothed_Fourier_drape_surface	Drape surface for Fourier reconstruction, smoothed flight surface	metres
Unsmoothed_Fourier_drape_surface	Drape surface for Fourier reconstruction, unsmoothed flight surface (actual flight surface)	metres
Fourier_gD_0_C	Fourier derived vertical gravity, no terrain correction applied, continuation applied	mGal
Fourier_gD_0_NC	Fourier derived vertical gravity, no terrain correction applied, no continuation applied	mGal
Fourier_gD_0_C_conformed	Fourier derived vertical gravity, no terrain correction applied, conformed to regional gravity, continuation applied	mGal
Fourier_gD_0_NC_conformed	Fourier derived vertical gravity, no terrain correction applied, conformed to regional gravity, no continuation applied	mGal
Fourier_GDD_0_C	Fourier derived vertical gravity gradient, no terrain correction applied, continuation applied	eotvos
Fourier_GDD_0_NC	Fourier derived vertical gravity gradient, no terrain correction applied, no continuation applied	eotvos
Fourier_gD_2_C	Fourier derived vertical gravity, terrain correction density 2 g/cm^3, continuation applied	mGal
Fourier_gD_2_NC	Fourier derived vertical gravity, terrain correction density 2 g/cm^3, no continuation applied	mGal
Fourier_gD_2_C_conformed	Fourier derived vertical gravity, terrain correction density 2 g/cm^3 conformed to regional gravity, continuation applied	mGal
Fourier_gD_2_NC_conformed	Fourier derived vertical gravity, terrain correction density 2 g/cm^3 conformed to regional gravity, no continuation applied	mGal
Fourier_GDD_2_C	Fourier derived vertical gravity gradient, terrain correction density 2 g/cm^3, continuation applied	eotvos
Fourier_GDD_2_NC	Fourier derived vertical gravity gradient, terrain correction density 2 g/cm^3, no continuation applied	eotvos
Fourier_gD_2p67_C	Fourier derived vertical gravity, terrain correction density 2.67 g/cm^3, continuation applied	mGal
Fourier_gD_2p67_NC	Fourier derived vertical gravity, terrain correction density 2.67 g/cm^3, no continuation applied	mGal
Fourier_gD_2p67_C_conformed	Fourier derived vertical gravity, terrain correction density 2.67 g/cm^3 conformed to regional gravity, continuation applied	mGal
Fourier_gD_2p67_NC_conformed	Fourier derived vertical gravity, terrain correction density 2.67 g/cm^3 conformed to regional gravity, no continuation applied	mGal
Fourier_GDD_2p67_C	Fourier derived vertical gravity gradient, terrain correction density 2.67 g/cm^3, continuation applied	eotvos
Fourier_GDD_2p67_NC	Fourier derived vertical gravity gradient, terrain correction density 2.67 g/cm^3, no continuation applied	eotvos

Table 4: Final AGG Grids – *Geosoft GRD Format*